

Symmetry Reduction and Rotation Numbers for Poncelet maps

H.E. Lomeli¹ and J. D. Meiss^{2*}

¹Department of Mathematics
University of Texas at Austin
Austin, TX 78712
lomeli@math.utexas.edu

²Department of Applied Mathematics
University of Colorado
Boulder, CO 80309-0526, USA
James.Meiss@colorado.edu

September 18, 2023

Abstract

Poncelet maps are circle maps constructed geometrically for a pair of nested ellipses; they are related to the classic billiard map on an elliptical domain when the orbit has an elliptical caustic. Here we show how the rotation number of the elliptical billiard map can be obtained from a symmetry generated from the flow of a pendulum Hamiltonian system. When such a symmetry flow has a global cross section, we previously showed that there are coordinates in which the map takes a reduced, skew-product form on a covering space. In particular, for elliptic billiard map this gives an explicit form for the rotation number of each orbit.

We show that the family Poncelet maps on a pencil of ellipses is conjugate to a corresponding family of billiard maps, and thus the Poncelet maps inherit the one-parameter family of continuous symmetries. Such a pencil has a single parameter, the *pencil eccentricity*, which becomes the modulus of the Jacobi elliptic functions used to construct a covering space that simultaneously simplifies all of the Poncelet maps. The rotation number of the Poncelet map for any element of a pencil can then be written in terms of elliptic functions as well. An implication is that the rotation number of the pencil has a monotonicity property: it is monotone increasing as the caustic ellipse shrinks.

The resulting expression for the rotation number gives an explicit condition for Poncelet porisms, the parameters for which the rotation number is rational. For such parameters, an orbit of the corresponding Poncelet map is periodic: it forms a polygon for *any* initial point. These universal parameters also solve the inverse problem: given a rotation number, which member of a pencil has a Poncelet map with that rotation number? Explicit conditions are given for a general rotation numbers and we see how they are related to Cayley's classic porism theorem.

Contents

1 Introduction	2
1.1 Elliptic billiards	3
1.2 Pencils of ellipses	4

*JDM was supported in part by NSF grants DMS-1812481 and CMMI-1537460.

1.3	Poncelet Porisms and Cayley conditions	6
1.4	Standard covering map and Full Poncelet Theorem	7
2	Confocal Ellipses and Billiard Maps	8
2.1	Billiards as Twist Maps	8
2.2	Symmetry Reduction of Elliptic Billiards	9
2.3	Poncelet Maps for Confocal Ellipses	11
3	Poristic Confocal Ellipses and Gauss symmetry	14
3.1	Poristic Parameters	14
3.2	Explicit Porisms	15
3.3	Half-Rotation Number	16
3.4	Gauss Symmetry	17
4	Pencils of Ellipses	18
4.1	Standing Assumptions	18
4.2	Simultaneous Diagonalization	20
4.3	Pencil Eccentricity	22
4.4	Projective Transformations	23
5	Poncelet maps for Pencils	24
5.1	Standard Pencil	24
5.2	Standard Covering Space	26
5.3	Explicit Rotation Number and Inverse Parameter Conditions	28
5.4	Monotonicity	32
6	Full Poncelet Theorem	33
7	Conclusions	36
A	Confocal Poristic Examples	37
A.1	Rotation number $\frac{1}{3}$	37
A.2	Cayley’s Solution for Period–5 orbits	37
B	Asymptotic Limits	38
C	Derivatives of the billiard rotation number	38

1 Introduction

Poncelet’s celebrated 1822 theorem [BKOR87, FT07, DR11, DR14] concerns polygons inscribed between a pair of ellipses: an “outer” ellipse, \mathcal{C}_o , that encloses an “inner” ellipse, \mathcal{C}_i . His theorem states that if there exists an n -sided polygon with all vertices on \mathcal{C}_o and all sides tangent to \mathcal{C}_i then for each $z \in \mathcal{C}_o$ there is also another n -sided polygon with z as a vertex that has the same properties. Associated with the pair $(\mathcal{C}_o, \mathcal{C}_i)$ there is a circle diffeomorphism on \mathcal{C}_o called the *Poncelet map* (or *Poncelet traverse* [NA12]). Indeed, for *any* pair of strictly convex curves $(\mathcal{C}_o, \mathcal{C}_i)$, with \mathcal{C}_i in the interior of \mathcal{C}_o , the homeomorphism

$$P : \mathcal{C}_o \rightarrow \mathcal{C}_o, \tag{1}$$

of the pair is defined so that for each $z_0 \in \mathcal{C}_o$, $z_1 = P(z_0)$ is the unique point on \mathcal{C}_o such that the segment $\overrightarrow{z_0 z_1}$ is tangent to \mathcal{C}_i with positive orientation, i.e., so that \mathcal{C}_i appears on the left when moving from z_0 to z_1 , see Fig. 1. Clearly there also exists a second point $z_{-1} \in \mathcal{C}_o$ such that $\overrightarrow{z_{-1} z_0}$ is also tangent to \mathcal{C}_i ; this point corresponds to the inverse of the map: $z_{-1} = P^{-1}(z_0)$.

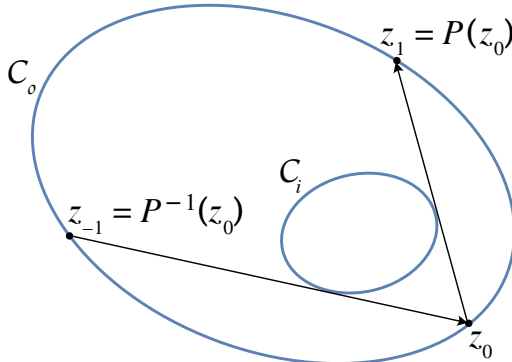


Figure 1: A Poncelet map $P : \mathcal{C}_o \rightarrow \mathcal{C}_o$ for a pair of nested, convex curves \mathcal{C}_o and \mathcal{C}_i .

Given an outer ellipse, the problem of characterizing the interior ellipses for which Poncelet polygons exist is called the problem of *Poncelet's porism*. The poristic case then corresponds to the existence of a periodic orbit of P . In its simplest version, Poncelet's theorem says that when \mathcal{C}_o and \mathcal{C}_i are ellipses, the existence of one period- n orbit implies that every orbit is period- n , i.e., that $P^n = \text{id}$ on \mathcal{C}_o : this map is idempotent.

When the curves are concentric circles, the proof of Poncelet's theorem is simple, and the family of polygons are simply obtained by rigid rotation about the common center of the circles, a symmetry of the circle. The proof of the general case has many versions, see e.g. [GH77, GH78, Kol85, CS10, CGM10, KKG10, BZ12, CM16]. In this paper we avoid using algebraic geometry (see e.g., [Fla09, DR11] for this approach) and concentrate on applying dynamical systems techniques.

Our first goal is to relate Poncelet's theorem to more general symmetries of integrable dynamical systems. We will argue that the theorem follows from the existence of an equivariant, continuous symmetry of P . In particular, this symmetry acts on a period- n orbit of P to deform it into a continuous family of orbits with the same period. Using this, we will address the fundamental problem of finding the rotation number of the Poncelet map generated by a pair of concentric ellipses.

Even when the Poncelet map is not poristic, its dynamics are conjugate to rigid rotation. In this paper, we find an explicit correspondence between the elements of a pencil of conics and rotation numbers. For a given pencil, we obtain a family of Poncelet maps that are uniquely identified by the rotation number. This correspondence can be written in terms of Jacobi elliptic functions that have a common modulus. The modulus is, in fact, an invariant of the pencil that we will call the pencil eccentricity.

1.1 Elliptic billiards

We will build the symmetry of P by conjugacy with the known symmetry of the elliptical billiard, which we recall in §2. We start with the family of ellipses with eccentricities $0 < \varepsilon < 1$ and foci at $(\pm 1, 0)$,

$$E(\varepsilon) = \left\{ (x, y) \in \mathbb{R}^2 : \varepsilon^2 x^2 + \left(\frac{\varepsilon^2}{1 - \varepsilon^2} \right) y^2 = 1 \right\} = \left\{ (x, y) \in \mathbb{R}^2 : \frac{x^2}{a^2} + \frac{y^2}{b^2} = 1 \right\}, \quad (2)$$

where $a = 1/\varepsilon$ and $b = \sqrt{1 - \varepsilon^2}/\varepsilon$ so that $0 < b < a$ and $a^2 - b^2 = 1$. For a given eccentricity $\varepsilon = f$, the billiard map, as studied by Birkhoff, is a symplectic twist map defined on the cotangent bundle of $E(f)$,

using the usual rule that the angle of incidence equals the angle of reflection. In this case, the outer ellipse is $\mathcal{C}_o = E(f)$. Orbits of the billiard map have caustics that are generically confocal ellipses or hyperbolas, see e.g., [CFS82, Ch. 6]. In §2.3 we recall the case that the caustic is an ellipse $\mathcal{C}_i = E(e)$ interior to \mathcal{C}_o with eccentricity e . Note that generally,

$$E(e) \subset \text{Int}(E(f)), \quad \text{whenever } 0 < f < e < 1.$$

This leads us to consider the triangle of eccentricity pairs

$$\Delta = \{(e, f) \in (0, 1) \times (0, 1) : f < e\}, \quad (3)$$

as sketched in Fig. 2. Whenever $(e, f) \in \Delta$, the orbits of the billiard map on $E(f)$ with caustic $E(e)$ induce a Poncelet map that we denote by

$$B_e^f : E(f) \rightarrow E(f).$$

We showed in [DLM12] that equivariant symmetries of maps are related to the existence of covering spaces when the symmetry flow has a global Poincaré section. In this case, the map has a lift to the covering space that takes a skew-product form. The billiard has an explicit symmetry that can be obtained from the flow of the pendulum, and this provides explicit forms for the universal cover and the skew-product lift.

A consequence is that when the caustic is an ellipse, the billiard map B_e^f restricted to each symmetry orbit is conjugate to a rigid rotation with a rotation number that we denote $\hat{\rho}(e, f)$. In §2.3, we show that the symmetry implies that this rotation number can be expressed using elliptic functions:

Theorem 1 (Billiard Rotation Number). *For each $(e, f) \in \Delta$, the rotation number $\hat{\rho}(e, f)$ of B_e^f is*

$$\hat{\rho}(e, f) = \frac{F(\hat{\omega}(e, f), e)}{2K(e)}, \quad \hat{\omega}(e, f) = \arcsin \sqrt{\frac{e^2 - f^2}{e^2(1 - f^2)}}, \quad (4)$$

where $F(\omega, e)$ is the incomplete elliptic integral of the first kind, (24), and $K(e) = F(\frac{\pi}{2}, e)$.

Versions of this standard result can also be found in [Kol85, CF88, RR14, DDCRR17, KS18].

The connection between general Poncelet maps and elliptic billiards allows us to find explicit expressions for the rotation number of the former as well. While there has been much written about this connection, e.g., [CF88, Tab93, DR98a, DR06, LT07, DR10, DR11, Gar19], as far as we know the equivariant billiard symmetry has not been previously used to analyze Poncelet maps.

1.2 Pencils of ellipses

When $(\mathcal{C}_o, \mathcal{C}_i)$ are a nested pair of ellipses, but are not confocal, the Poncelet map as sketched in Fig. 1 is not the billiard map on \mathcal{C}_o : the usual equality of the angle of reflection and the angle of incidence is abandoned. Nevertheless, P is still a circle homeomorphism on \mathcal{C}_o , and thus, as shown by Poincaré, every orbit has a rotation number. In §4 we recall that a general ellipse \mathcal{C} is associated with a 3×3 symmetric matrix C using projective coordinates so that

$$\mathcal{C} = \{(x, y) \in \mathbb{R}^2 : \mathbf{u}^T C \mathbf{u} = 0, \mathbf{u} = (x, y, 1)^T\}. \quad (5)$$

The assumptions on the matrix C so that the associated curve \mathcal{C} is an ellipse are given in §4.1.

Given a fixed pair of nested ellipses $\mathcal{C}_1, \mathcal{C}_2$ for which $\mathcal{C}_2 \subset \text{Int}(\mathcal{C}_1)$ and their associated matrices C_1, C_2 , a *pencil* is the one-parameter family generated by linear combinations of the implicit equations:

$$\mathcal{C}_\nu = \{(x, y) \in \mathbb{R}^2 : \mathbf{u}^T (\nu_1 C_1 + \nu_2 C_2) \mathbf{u} = 0, \mathbf{u} = (x, y, 1)^T\}, \quad (6)$$

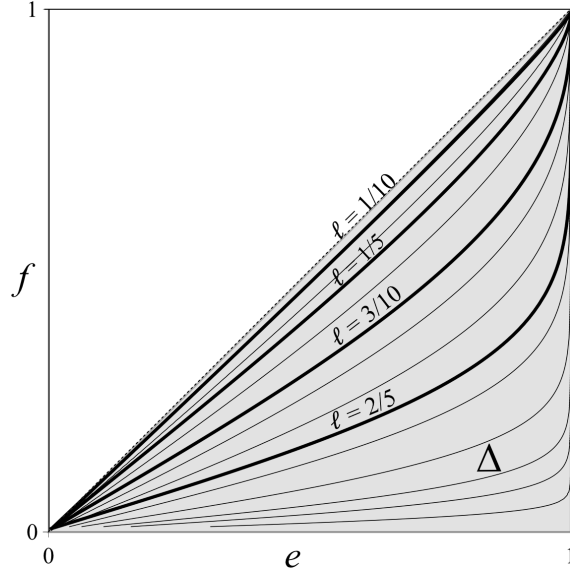


Figure 2: Level sets of the rotation number (4) (curves) defined on the set Δ (3) (gray). The zero set of the Cayley polynomial, Cay_{10} given by (12), has four connected components, each corresponding to a poristic curve Δ_ℓ with $\hat{\rho}(e, f) = \ell$ for $\ell = 1/10, 1/5, 3/10,$ and $2/5$.

where the parameters $\nu = (\nu_1, \nu_2)$ determine the element of the pencil.

We show in §4.2 that under natural assumptions the associated matrices C_1 and C_2 can simultaneously diagonalized by a congruency, and we can choose this transformation so that the outer ellipse becomes the unit circle in the new coordinates. Many of the properties of the Poncelet map $P : \mathcal{C}_1 \rightarrow \mathcal{C}_1$ with inner caustic \mathcal{C}_2 are determined by the eigenvalues $\lambda_1, \lambda_2,$ and λ_3 of the matrix $C_1^{-1}C_2$. We show that these can be ordered so that

$$\lambda_1 > \lambda_2 > \lambda_3 > 0.$$

For such eigenvalues, \mathcal{C}_ν is an ellipse interior to \mathcal{C}_1 and satisfies the standing assumptions of §4.1 precisely when the vector $\nu = (\nu_1, \nu_1)$ is in the cone

$$\nu_2 > 0 \text{ and } \nu_1 + \lambda_3\nu_2 > 0, \tag{7}$$

as illustrated below in Fig. 9.

Given pencil eigenvalues as above, we define in §4.3 the *pencil eccentricity* for (6) as

$$e(\mathcal{C}_1, \mathcal{C}_2) \equiv \sqrt{\frac{\lambda_1 - \lambda_2}{\lambda_1 - \lambda_3}}. \tag{8}$$

We show in Lem. 16 that this eccentricity is a pencil invariant: for a fixed outer ellipse, (8) is the same for any inner ellipse \mathcal{C}_ν : $e(\mathcal{C}_1, \mathcal{C}_2) = e(\mathcal{C}_1, \mathcal{C}_\nu)$.

Moreover, we show in §4.4 that the diagonalization transformation can be thought of as a projective diffeomorphism that maps the general pencil (6) into a *standard* pencil, see §5.1, for which the outer curve becomes the unit circle.

Fixing parameters $\nu = (\nu_1, \nu_2)$ as in (7), we denote the Poncelet map for the outer ellipse $\mathcal{C}_o = \mathcal{C}_1$ and inner caustic $\mathcal{C}_i = \mathcal{C}_\nu$ (6) by

$$P_\nu : \mathcal{C}_1 \rightarrow \mathcal{C}_1. \tag{9}$$

If e is the pencil eccentricity (8), we can construct a conjugacy between P_ν and the billiard map B_e^f for a given f that is a function only of e , the eigenvalues, and ν (see (55)). A sketch of the conjugacy, Fig. 3,

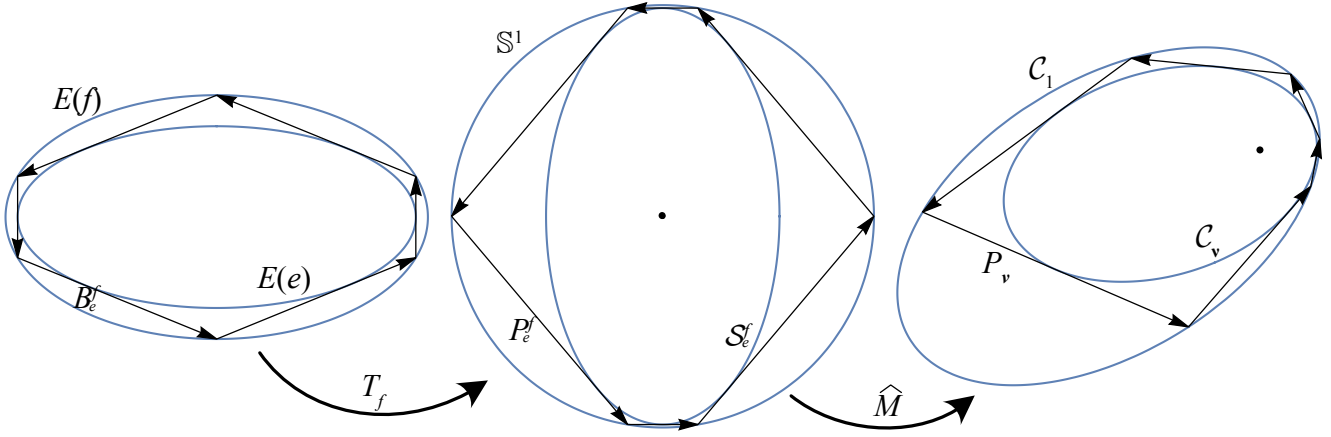


Figure 3: Conjugacy between the billiard circle map B_e^f , the standard Poncelet map P_e^f (54) for which the outer curve is a circle, and a general Poncelet map P_ν . Here the eccentricities are $e = \sqrt{\frac{27}{32}} \approx 0.918559$ and $f = \frac{\sqrt{3}}{2} \approx 0.866025$ and the eigenvalues are $(\lambda_1, \lambda_2, \lambda_3) = (\frac{1}{5}, \frac{1}{8}, \frac{1}{9})$.

uses the standard pencil as an intermediary. In §5 we show that this connects the rotation number (4) of the billiard map B_e^f to that of more general Poncelet maps, leading—in §5.2—to the following theorem.

Theorem 2 (Poncelet Rotation Number). *If \mathcal{C}_ν is a pencil with eigenvalues $\lambda_1, \lambda_2, \lambda_3$ and eccentricity e (8), then for each valid ν (7) the rotation number of the corresponding Poncelet map (9) is*

$$\rho(\nu) = \frac{F(\omega(\nu), e)}{2K(e)}, \quad \omega(\nu) = \omega(\nu_1, \nu_2) = \arcsin \sqrt{\frac{(\lambda_1 - \lambda_3)\nu_2}{\lambda_1\nu_2 + \nu_1}}. \quad (10)$$

This relation allows the computation of the rotation number for a general Poncelet map for ellipses in a pencil knowing only the eigenvalues of the matrix $C_1^{-1}C_2$. Note that the modulus of these elliptic functions is fixed and equal to the pencil eccentricity and that ρ_ν is a homogeneous function of the components of ν .

In §5.4 we prove that Poncelet maps and the rotation number (10) satisfy a monotonicity property:

Theorem 3 (Monotonicity). *Suppose \mathcal{C}_ν and \mathcal{C}_μ are ellipses in a pencil (6) with parameters ν and μ satisfying (7) so that both are in the interior of an outer ellipse \mathcal{C}_1 . If $\rho(\mu)$ and $\rho(\nu)$ are the rotation numbers (10) of the corresponding maps P_μ , and P_ν , then the following are equivalent:*

- 1) $\mathcal{C}_\mu \subset \text{Int}(\mathcal{C}_\nu)$,
- 2) $\nu \times \mu > 0$,
- 3) $\rho(\mu) > \rho(\nu)$.

In particular, this shows that the rotation number is a monotonically increasing function as the inner caustic shrinks in the pencil. In the limit when the inner ellipse becomes a point (e.g., $\nu_1 + \lambda_3\nu_2 = 0$) and the rotation number becomes $\rho(\nu) = \frac{1}{2}$ as illustrated in Fig. 9.

1.3 Poncelet Porisms and Cayley conditions

As we recall in §3, the Poncelet porism problem for the confocal case is equivalent to finding a pair of eccentricities $(e, f) \in \Delta$ for which $\hat{\rho}(e, f) \in \mathbb{Q}$. Using the form (4), we find in §3.2 an explicit parameterization of the curve $\Delta_\ell \subset \Delta$ of parameters for which $\hat{\rho}(e, f) = \ell \in [0, \frac{1}{2}]$, rational or irrational; the latter correspond to quasi-periodic orbits of B_e^f . Several examples can be seen in Fig. 2.

Subsets of Δ for which the orbit of a Poncelet map has period N were found by Cayley, see e.g. [GH78, DR98a, Fla09, Mir10, Mir12, NA12, CS10, GR21]. Though the Cayley conditions do not explicitly give the rotation number, they are a useful first step in identifying poristic ellipses. We argue below that the rotation number is a better tool.

For each $N > 2$, Cayley found a polynomial, Cay_N , with the property that the Poncelet map has a periodic orbit with period dividing N if and only if $\text{Cay}_N = 0$. This method uses the expansion of the square root of the generalized characteristic polynomial,

$$\sqrt{\det(\lambda C_1 - C_2)} = \alpha_0 + \alpha_1 \lambda + \alpha_2 \lambda^2 + \dots, \quad (11)$$

where C_1 and C_2 are matrices representing the ellipses \mathcal{C}_1 and \mathcal{C}_2 , respectively, and we require that $\det(C_2) < 0$. For confocal ellipses, the coefficients α_j are rational functions in the eccentricities e and f and the Cayley condition $\text{Cay}_N(\alpha_2, \dots, \alpha_{N-1}) = 0$ can be written as a polynomial in (e, f) .

Note that $\text{Cay}_N = 0$ implies that $\hat{\rho}(e, f) = k/N$, for some $0 < k < N/2$; however, since the zero set necessarily includes each such rotation number the equations become unmanageable very fast. Finding the factors of the Cayley polynomial for each $\Delta_{k/N}$ is practical only for small values of N . For example, for a pair of confocal ellipses the Cayley condition for $N = 10$ has the form

$$\text{Cay}_{10}(\alpha_2, \dots, \alpha_9) = \begin{pmatrix} \alpha_3 & \alpha_4 & \alpha_5 & \alpha_6 \\ \alpha_4 & \alpha_5 & \alpha_6 & \alpha_7 \\ \alpha_5 & \alpha_6 & \alpha_7 & \alpha_8 \\ \alpha_6 & \alpha_7 & \alpha_8 & \alpha_9 \end{pmatrix} = 0.$$

The resulting set includes all the pairs $(e, f) \in \Delta$ for which the billiard rotation number $\hat{\rho}(e, f) = \frac{1}{10}, \frac{1}{5}, \frac{3}{10}$, or $\frac{2}{5}$, i.e.,

$$(\text{Cay}_{10})^{-1}\{0\} \cap \Delta = \Delta_{1/10} \cup \Delta_{1/5} \cup \Delta_{3/10} \cup \Delta_{2/5}. \quad (12)$$

Thus the Cayley set splits into four components labelled by rotation number, as shown by the thicker curves in Fig. 2. We recall several additional explicit examples in §3.1 and App. A.

By contrast, the explicit expression (4) allows us to solve the inverse problem and directly parameterize each set Δ_ℓ : given a rotation number ℓ and one of the eccentricities e or f , find the other eccentricity. In particular, we will show in Lem. 10 that, for all $\ell \in (0, 1/2)$, $\hat{\rho}(e, f) = \ell$ if and only if $f = e \text{cd}(2K(e)\ell, e)$, for the Jacobi elliptic function cd . In §5.3 we generalize this result to an arbitrary pencil (6), giving a complete solution of the inverse problem:

Theorem 4 (Inverse parameter conditions). *The Poncelet map (9) with pencil eccentricity (8) has rotation number $\rho(\nu) = \ell \in (0, \frac{1}{2})$ if and only if (ν_1, ν_2) lie on the ray*

$$\frac{\nu_1}{\nu_2} = \frac{\lambda_1 \text{cn}^2(2K(e)\ell, e) - \lambda_3}{\text{sn}^2(2K(e)\ell, e)} \quad (13)$$

in the cone of parameters (7).

The remarkable feature of this result is that we can determine the element of the pencil whose Poncelet map has a given rotation number using only the eigenvalues of $C_1^{-1}C_2$: the explicit conjugacy to the billiard map is not needed.

1.4 Standard covering map and Full Poncelet Theorem

As another consequence of the results of §4, we will find a covering space that simultaneously simplifies all the Poncelet maps in §5. Let \mathcal{C}_ν be a pencil generated by two matrices C_1, C_2 that satisfy the standing

assumptions (SA1)-(SA3). In §5.2, we show that there exists a covering map $\Pi_M : \mathbb{R} \rightarrow \mathcal{C}_1$ such that each Poncelet map $P_\nu : \mathcal{C}_1 \rightarrow \mathcal{C}_1$ has a lift of the form $B_\nu(\theta) = \theta + \rho(\nu)$, where $\rho(\nu)$ is the rotation number (10). This is shown in the following commutative diagram.

$$\begin{array}{ccc} \mathbb{R} & \xrightarrow{B_\nu} & \mathbb{R} \\ \Pi_M \downarrow & & \downarrow \Pi_M \\ \mathcal{C}_1 & \xrightarrow{P_\nu} & \mathcal{C}_1 \end{array}$$

We will see that the covering map Π_M depends only on the eccentricity of the pencil and the matrix that simultaneously diagonalizes C_1 and C_2 .

In §6 we generalize these results to a Poncelet map (1) with a sequence of inner ellipses \mathcal{C}_ν in a given pencil. We will see that the corresponding Poncelet maps commute. Using this, we obtain a more general version of Poncelet's theorem with multiple inner ellipses.

Theorem 5. *Suppose that $\nu^1, \nu^2, \dots, \nu^N$ is a finite sequence of parameters satisfying (7), and that $\mathcal{C}_{\nu^1}, \dots, \mathcal{C}_{\nu^N}$ are the corresponding inner ellipses in the pencil. Then the circle map on \mathcal{C}_1 defined by the composition*

$$P_* = (P_{\nu^N})^{k_N} \circ (P_{\nu^{N-1}})^{k_{N-1}} \circ \dots \circ (P_{\nu^1})^{k_1}, \quad (14)$$

for $k_1, k_2, \dots, k_N \in \mathbb{Z}$, has the rotation number

$$\rho(P_*) = k_1 \rho(\nu^1) + k_2 \rho(\nu^2) + \dots + k_N \rho(\nu^N),$$

where $\rho(\nu)$ is given by (10). In particular, if the rotation number of (14) is an integer, $\rho(P_*) \in \mathbb{Z}$, then $P_* = id$. Similarly, if P_* has a fixed point then $\rho(P_*) \in \mathbb{Z}$ and hence $P_* = id$.

2 Confocal Ellipses and Billiard Maps

We start with the simplest case: the Poncelet map P for a pair of confocal ellipses. In this case, we will see that P corresponds to an orbit of the billiard map with boundary $\mathcal{C}_o = E(f)$ that has the inner ellipse $\mathcal{C}_i = E(e)$ as a caustic with $0 < f < e < 1$. We recall in §2.1 the twist map formulation for billiard maps, and then, in §2.2, specialize to the integrable, elliptic case. The elliptic billiard has a symmetry that is a Hamiltonian flow and allows us to apply a theorem from [DLM12]. This theorem shows how to lift a map with a symmetry to a covering space on which it has a semi-direct product form. These results will be applied to the confocal Poncelet map in §2.3.

2.1 Billiards as Twist Maps

Classical billiard twist-map dynamics on smooth, convex curve \mathcal{C} gives rise to a twist map of an annulus. To recall this, let $\gamma : \mathbb{R} \rightarrow \mathbb{R}^2$ be a 2π -periodic,¹ parametric representation of \mathcal{C} :

$$\mathcal{C} = \{\gamma(\varphi) \in \mathbb{R}^2 : \varphi \in \mathbb{R}/2\pi\mathbb{Z}\}. \quad (15)$$

If $S(\varphi_0, \varphi_1) = \|\gamma(\varphi_0) - \gamma(\varphi_1)\|$ denotes the Euclidean length of a line segment from $\gamma(\varphi_0)$ to $\gamma(\varphi_1)$, then an orbit of the billiard consists of a sequence $\{\dots, \varphi_k, \varphi_{k+1}, \dots\}$ so that the formal orbit length,

$$W(\dots, \varphi_0, \varphi_1, \varphi_2, \dots) = \sum_{k \in \mathbb{Z}} S(\varphi_{k-1}, \varphi_k),$$

¹The twist map structure does not depend on having 2π -periodicity, but we can assume this without loss of generality. As an alternative one could use the arc length to parameterize the curve [Mei92].

is stationary with respect to variations of φ_k . This is, for all $k \in \mathbb{Z}$,

$$\frac{\partial S}{\partial \varphi_1}(\varphi_{k-1}, \varphi_k) + \frac{\partial S}{\partial \varphi_0}(\varphi_k, \varphi_{k+1}) = 0.$$

Equivalently, one can define a canonically conjugate ‘‘momentum’’ variable r , so that the two definitions,

$$\begin{aligned} r_0(\varphi_0, \varphi_1) &= -\frac{\partial S}{\partial \varphi_0}(\varphi_0, \varphi_1) = \frac{\langle \gamma(\varphi_1) - \gamma(\varphi_0), \gamma'(\varphi_0) \rangle}{S(\varphi_0, \varphi_1)}, \\ r_1(\varphi_0, \varphi_1) &= \frac{\partial S}{\partial \varphi_1}(\varphi_0, \varphi_1) = \frac{\langle \gamma(\varphi_1) - \gamma(\varphi_0), \gamma'(\varphi_1) \rangle}{S(\varphi_0, \varphi_1)}, \end{aligned}$$

agree along an orbit: $r_0(\varphi_k, \varphi_{k+1}) = r_1(\varphi_{k-1}, \varphi_k)$. These definitions imply the standard rule that the ‘‘angle of incidence’’ is equal to the ‘‘angle of reflection’’.

Letting $\mathcal{M} = \{(\varphi_0, \varphi_1) \in \mathbb{R}/2\pi\mathbb{Z} \times \mathbb{R}/2\pi\mathbb{Z} : \varphi_0 \neq \varphi_1\}$, the Lagrangian form of the billiard map $L : \mathcal{M} \rightarrow \mathcal{M}$, is

$$(\varphi_k, \varphi_{k+1}) = L(\varphi_{k-1}, \varphi_k).$$

Alternatively, the canonical form of this map is defined on the open annulus

$$\mathbb{A} = \{(\varphi, r) \in \mathbb{R}/2\pi\mathbb{Z} \times \mathbb{R} : r^2 < \|\gamma'(\varphi)\|^2\}. \quad (16)$$

To obtain this, first define two functions $\kappa_{0,1} : \mathcal{M} \rightarrow \mathbb{A}$ by

$$\begin{aligned} \kappa_0(\varphi_0, \varphi_1) &= (\varphi_0, r_0(\varphi_0, \varphi_1)), \\ \kappa_1(\varphi_0, \varphi_1) &= (\varphi_1, r_1(\varphi_0, \varphi_1)). \end{aligned} \quad (17)$$

When \mathcal{C} is strictly convex and γ is C^2 , these can be shown to be diffeomorphisms [Lom96]. The canonical billiard map $B : \mathbb{A} \rightarrow \mathbb{A}$ is then given by $B = \kappa_1 \circ \kappa_0^{-1}$, so that

$$(\varphi_{k+1}, r_{k+1}) = B(\varphi_k, r_k). \quad (18)$$

Note that $L = \kappa_1^{-1} \circ \kappa_0^{-1} = \kappa_0^{-1} \circ B \circ \kappa_0$, so that L is conjugate to B . This construction implies that B is symplectic with respect to the two-form $\Omega = d\varphi \wedge dr$. Indeed, B is the exact symplectic twist map generated by $S(\varphi_0, \varphi_1)$ [Mei92, Lom96].

2.2 Symmetry Reduction of Elliptic Billiards

Suppose that the billiard has boundary $\mathcal{C} = E(f)$, (2), for some $0 < f < 1$. Following (15), the ellipse has the convenient parameterization

$$E(f) = \left\{ \gamma(\varphi) = \frac{1}{f}(\cos \varphi, \sqrt{1-f^2} \sin \varphi) \in \mathbb{R}^2 : 0 \leq \varphi < 2\pi \right\}. \quad (19)$$

Noting that $\|\gamma'(\varphi)\|^2 = \frac{1}{f^2}(1-f^2 \cos^2 \varphi)$, then the annulus (16) becomes

$$\mathbb{A} = \left\{ (\varphi, r) \in (\mathbb{R}/2\pi\mathbb{Z}) \times \mathbb{R} : H(\varphi, r) < \frac{1}{2}f^{-2} \right\},$$

where

$$H(\varphi, r) = \frac{1}{2}r^2 + \frac{1}{2}\cos^2 \varphi. \quad (20)$$

As is well known, [Lom96], H is an invariant under the elliptic billiard dynamics: $B^*H = H$; thus the orbits of (18) lie on contours of H , as shown in Fig. 4. The associated symmetry is the Hamiltonian vector field X_H generated by H with respect to Ω , i.e., the function that satisfies $i_{X_H}\Omega = dH$. To see this, let $\Phi : \mathbb{R} \times \mathbb{A} \rightarrow \mathbb{A}$ be the (complete) flow of X_H . Writing $\Phi_t = \Phi(t, \cdot)$, as usual, then

$$\frac{\partial}{\partial t} \Phi_t(\xi) = X_H(\Phi_t(\xi)), \quad X_H(\Phi_t) = (H_r(\Phi_t), -H_\varphi(\Phi_t)), \quad \Phi_0(\xi) = \xi.$$

Lemma 6. Φ_t is an equivariant symmetry for the map $B: B \circ \Phi_t = \Phi_t \circ B$, for all $t \in \mathbb{R}$.

Proof. Since B is symplectic, then $B^*\Omega = \Omega$. Since $H = B^*H$, then

$$i_{X_H}\Omega = dH = d(B^*H) = B^*(i_{X_H}\Omega) = i_{B^*X_H}\Omega,$$

so $B^*X_H = X_H$. This implies that the flow Φ_t commutes with the map B . □

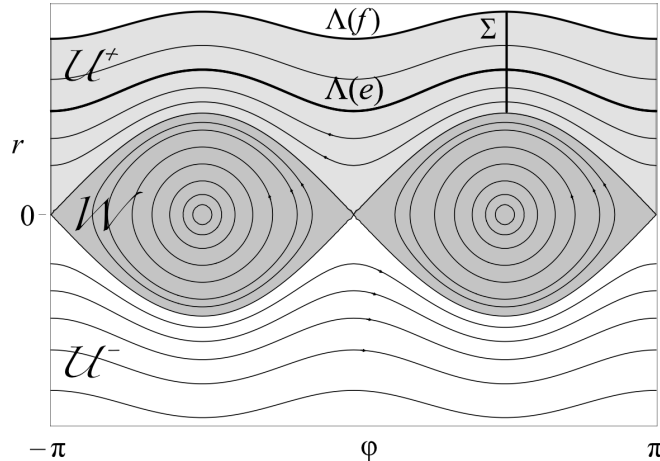


Figure 4: Contours (20) of the invariant H in the annulus \mathbb{A} , showing the sets \mathcal{U}^\pm , \mathcal{W} and its boundary \mathcal{V} . The Poincaré section $\Sigma = \{\varphi = \pi/2\} \cap \mathcal{U}^+$ is indicated by the vertical segment. The invariant sets $\Lambda(f)$ and $\Lambda(e)$ are labeled.

The phase space \mathbb{A} can be divided into four invariant subsets as shown in Fig. 4: $\mathcal{V} = \{H = \frac{1}{2}\}$, $\mathcal{W} = \{0 \leq H < \frac{1}{2}\}$, $\mathcal{U}^+ = \{\frac{1}{2} < H < \frac{1}{2}f^{-2}, r > 0\}$, and $\mathcal{U}^- = \{\frac{1}{2} < H < \frac{1}{2}f^{-2}, r < 0\}$.

The set \mathcal{W} contains the period two orbit $(-\frac{\pi}{2}, 0) \rightarrow (\frac{\pi}{2}, 0)$; more generally, its two components are mapped from one to the other under B . However, note that Φ leaves each component of \mathcal{W} invariant. The boundary set \mathcal{V} separates \mathcal{W} from the outside regions \mathcal{U}^\pm ; it consists of orbits that are homoclinic to the period-two saddle $(0, 0) \rightarrow (\pi, 0)$.

In this paper, we will consider only the dynamics of B restricted to \mathcal{U}^+ where the orbits encircle the ellipse in a counter-clockwise direction. As is well-known, the orbits of the elliptic billiard in \mathcal{U}^+ have caustics that are ellipses [CF88, Lom96, DR10]. Each level set of H in \mathcal{U}^+ is a topological circle that we will denote by

$$\Lambda(e) = \{(\varphi, r) \in \mathcal{U}^+ : H(\varphi, r) = \frac{1}{2}e^{-2}\}, \quad (21)$$

where e is the eccentricity of the ellipse $E(e)$ that is the corresponding caustic.

Thus, if $(\varphi_0, r_0) \in \Lambda(e)$, then the bi-infinite orbit $(\varphi_k, r_k) = B^k(\varphi_0, r_0)$ has the property that each segment $\overrightarrow{\gamma(\varphi_k)\gamma(\varphi_{k+1})}$ is tangent to the caustic $E(e)$. Then \mathcal{U}^+ is foliated by these level sets: $\mathcal{U}^+ = \bigcup\{\Lambda(e) : f < e < 1\}$. The dynamics on \mathcal{U}^- are similar under a reflection.

As we will see below, Poncelet's theorem can be viewed as a consequence of a lifting theorem for equivariant maps that we proved in [DLM12]. To apply this theorem, let

$$\Sigma = \left\{ \left(\frac{\pi}{2}, r \right) \in \mathbb{R}^2 : 1 < r < \frac{1}{f} \right\} = \{\varphi = \frac{\pi}{2}\} \cap \mathcal{U}^+, \quad (22)$$

be a (complete) Poincaré section for the flow Φ_t on the invariant set \mathcal{U}^+ , as indicated in Fig. 4.

Theorem 7 (Equivariant Lifting). *The map $p_0 : \mathbb{R} \times \Sigma \rightarrow \mathcal{U}^+$ defined by $p_0(t, \xi) = \Phi_t(\xi)$ is a covering map, with a cyclic group of deck transformations generated by $\psi(t, \xi) = (t + T(\xi), \xi)$, where $T(\xi)$ is the period of $\Phi_t(\xi)$. In addition, the lift of the billiard map $B|_{\mathcal{U}^+}$, $\tilde{B} : \mathbb{R} \times \Sigma \rightarrow \mathbb{R} \times \Sigma$, is*

$$\tilde{B}(t, \xi) = (t + \hat{\rho}(\xi), \xi), \quad (23)$$

where $\hat{\rho} : \Sigma \rightarrow \mathbb{R}$ is a smooth function on Σ .

Proof. The manifold Σ is simply connected and relatively closed in \mathcal{U}^+ . Previously [DLM12], we argued that such conditions imply that p_0 is a covering map, with deck transformations generated by $\psi(\xi, \theta) = (\Phi_{-T(\xi)}(\xi), \theta + T(\xi))$, where T is the smallest positive time such that $\Phi_{T(\xi)}(\xi) \in \Sigma$. Since the flow $\Phi_t(\xi)$ is periodic, $T(\xi)$ is the period of $\Phi_t(\xi)$, and $\Phi_{-T(\xi)}(\xi) = \xi$.

It was also proven in [DLM12] that, under the covering space p_0 , the lift \tilde{B} of any diffeomorphism B that is equivariant with respect to Φ_t has to have the skew product form $\tilde{B}(t, e) = (t + \hat{\rho}(e), g(e))$, where $g : \Sigma \rightarrow \Sigma$ is a diffeomorphism of Σ . In this case, the invariance of each level set implies that $g(e) = e$, giving (23). \square

2.3 Poncelet Maps for Confocal Ellipses

As in §1.1, we denote the Poncelet map for the confocal ellipses by B_e^f , to indicate that it is conjugate to the billiard map restricted to the invariant set $\Lambda(e)$, defined in (21).

Lemma 8 (Confocal Poncelet Map). *Given eccentricities $0 < f < e < 1$, let $B_e^f : E(f) \rightarrow E(f)$ denote the Poncelet map with respect to the confocal ellipses $E(f)$ and $E(e)$. Then B_e^f is conjugate to the elliptical billiard map $B|_{\Lambda(e)}$, i.e., the billiard map for the boundary $E(f)$ restricted to orbits with positive orientation that have $E(e)$ as a caustic.*

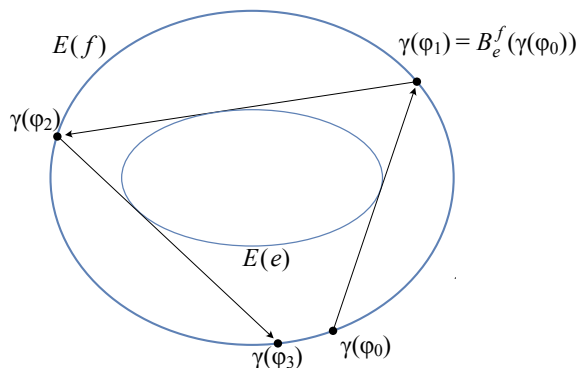


Figure 5: Confocal Poncelet map B_e^f on $E(f)$ with caustic $E(e)$.

Proof. Fixing $0 < f < 1$, we parameterize $E(f)$ using $\gamma : \mathbb{S}^1 \rightarrow \mathbb{R}^2$ as in (19). As sketched in Fig. 5, if $(\varphi_k, r_k) = B^k(\varphi_0, r_0)$ is the billiard orbit for $(\varphi_k, r_k) \in \Lambda(e)$, then each point $z_k = \gamma(\varphi_k) \in E(f)$, and each oriented segment $\overrightarrow{z_k z_{k+1}}$ is tangent to $E(e)$ with positive orientation. This implies that $B_e^f(\gamma(\varphi_k)) = z_{k+1} = \gamma(\varphi_{k+1})$, for all $k \in \mathbb{Z}$. Thus the Poncelet map B_e^f is conjugate to the elliptic billiard map $B|_{\Lambda(e)}$. \square

It is this link between the elliptical billiard and Poncelet maps that we will use in the following sections to study general Poncelet maps.

Remark 1. To define several of the covering spaces that will reveal the structure of Poncelet maps, we use the Jacobi elliptic functions sn , cn , dn and am with modulus e . These have period $4K(e)$, where $K(e) = F(\frac{\pi}{2}, e)$ is the complete elliptic integral of the first kind, and

$$F(\phi, e) \equiv \int_0^\phi \frac{d\tau}{\sqrt{1 - e^2 \sin^2 \tau}}. \quad (24)$$

Theorem 9 (Confocal Covering Map). *For $0 < f < e < 1$, the map $\pi_e^f : \mathbb{R} \rightarrow E(f)$ defined by*

$$\pi_e^f(\theta) = \frac{1}{f} \left(\begin{array}{c} -\text{sn}(4K(e)\theta, e) \\ \sqrt{1 - f^2} \text{cn}(4K(e)\theta, e) \end{array} \right), \quad (25)$$

is a covering map of $E(f)$, with group of deck transformations generated by $\theta \mapsto \theta + 1$. Moreover, the Poncelet map B_e^f has a lift of the form

$$\tilde{B}_e^f(\theta) = \theta + \hat{\rho}(e, f), \quad (26)$$

where $\hat{\rho}(e, f)$ only depends on (e, f) . In addition, we can assume that $0 < \hat{\rho}(e, f) < 1$.

Proof. An explicit formula for the lift $p_0 : \mathbb{R} \times \Sigma \rightarrow \mathcal{U}^+$ of Thm. 7 can be obtained using properties of Jacobi elliptic functions. Letting $\xi = (\frac{\pi}{2}, r) \in \Sigma$, (22), then the explicit form of the flow of the pendulum, see e.g., [Och11], implies that

$$p_0(t, \xi) = \Phi_t(\xi) = \left(\begin{array}{c} \text{am}(rt, r^{-1}) + \pi/2 \\ r \text{dn}(rt, r^{-1}) \end{array} \right). \quad (27)$$

To specialize this to the level set $\Lambda(e) \subset \mathcal{U}^+$, we let $\xi_e = (\pi/2, e^{-1}) = \Sigma \cap \Lambda(e)$, and $q_e : \mathbb{R} \rightarrow \Lambda(e)$ be the function

$$q_e(\theta) \equiv p_0(4eK(e)\theta, \xi_e) = \left(\begin{array}{c} \text{am}(4K(e)\theta, e) + \pi/2 \\ e^{-1} \text{dn}(4K(e)\theta, e) \end{array} \right). \quad (28)$$

We define the inclusion $i : \Lambda(e) \hookrightarrow \mathcal{U}^+$, and the embedding $j : \mathbb{R} \rightarrow \mathbb{R} \times \Sigma$ given by $j(\theta) = (4eK(e)\theta, \xi_e)$. The implication is that the range of $p_0 \circ j$ is $\Lambda(e)$, and that the following diagram commutes:

$$\begin{array}{ccc} \mathbb{R} & \xrightarrow{j} & \mathbb{R} \times \Sigma \\ q_e \downarrow & & \downarrow p_0 \\ \Lambda(e) & \xrightarrow{i} & \mathcal{U}^+ \end{array}$$

In other words, $i \circ q_e = p_0 \circ j$. This implies that q_e is a covering map of $\Lambda(e)$. A simple computation shows that $B|_{\Lambda(e)}$, the billiard map restricted to the level set $\Lambda(e)$, obeys

$$B|_{\Lambda(e)} \circ q_e(\theta) = q_e(\theta + \hat{\rho}(e, f)), \quad (29)$$

for all θ , where $\hat{\rho}(e, f) = \hat{\rho}(\xi_e)/(4K(e))$. This shows that $\tilde{B}_e^f(\theta) = \theta + \hat{\rho}(e, f)$ is a lift of $B|_{\Lambda(e)}$.

We let $J_f : \Lambda(e) \rightarrow E(f)$ be the diffeomorphism $J_f(\varphi, r) = \frac{1}{f}(\cos \varphi, \sqrt{1 - f^2} \sin \varphi)$. Then the composition $J_f \circ q_e$ is a covering map of $E(f)$, and $\pi_e^f = J_f \circ q_e$. Note that the circle map B_e^f satisfies

$J_f \circ B|_{\Lambda(e)} = B_e^f \circ J_f$. The implication is that the diagram

$$\begin{array}{ccc}
\mathbb{R} & \xrightarrow{\tilde{B}_e^f} & \mathbb{R} \\
q_e \downarrow & & \downarrow q_e \\
\Lambda(e) & \xrightarrow{B|_{\Lambda(e)}} & \Lambda(e) \\
J_f \downarrow & & \downarrow J_f \\
E(f) & \xrightarrow{B_e^f} & E(f)
\end{array}
\begin{array}{l}
\pi_e^f \curvearrowright \\
\pi_e^f \curvearrowleft
\end{array}$$

commutes. This also implies that the map \tilde{B}_e^f , given by (26), is a lift of B_e^f to the covering map π_e^f . Given that the group of deck transformations is generated by $\theta \mapsto \theta + 1$, we can assume that $0 < \hat{\rho}(e, f) < 1$. \square

By (26), the rotation number of B_e^f is $\hat{\rho}(e, f)$. We can now prove that this is given by (4), the result mentioned in §1:

Proof of Thm. 1 (Billiard Rotation Number). Suppose $(e, f) \in \Delta$ and fix $\omega = \hat{\omega}(e, f)$ as in (4). Since $0 < f < e < 1$, $0 < \omega < \pi/2$. Using the annular coordinates (16), we define

$$\varphi_0 = \frac{\pi}{2} - \omega, \quad \varphi_1 = \frac{\pi}{2} + \omega, \quad r_0 = e^{-1} \sqrt{1 - e^2 \sin^2(\omega)}. \quad (30)$$

Since $H(\varphi_0, r_0) = H(\varphi_1, r_0) = \frac{1}{2}e^{-2}$, and $r_0 > 0$, it is clear that $(\varphi_0, r_0), (\varphi_1, r_0) \in \Lambda(e)$. Moreover, using (17) we have that $\kappa_0(\varphi_0, \varphi_1) = (\varphi_0, r_0)$ and $\kappa_1(\varphi_0, \varphi_1) = (\varphi_1, r_0)$. The implication is that $B|_{\Lambda(e)}(\varphi_0, r_0) = (\varphi_1, r_0)$.

Letting

$$\theta_1 = -\theta_0 = \frac{F(\omega, e)}{4K(e)}, \quad (31)$$

then from (28), usual identities for Jacobi elliptic functions imply that $q_e(\theta_0) = (\varphi_0, r_0)$ and $q_e(\theta_1) = (\varphi_1, r_0)$. We know that \tilde{B}_e^f is of the form (26) with $0 < \hat{\rho}(e, f) < 1$. Moreover, (29) implies that $q_e \circ \tilde{B}_e^f = B|_{\Lambda(e)} \circ q_e$, and thus

$$q_e \left(\tilde{B}_e^f(\theta_0) \right) = B|_{\Lambda(e)}(q_e(\theta_0)) = B|_{\Lambda(e)}(\varphi_0, r_0) = (\varphi_1, r_0) = q_e(\theta_1).$$

Therefore, there exists an integer $m \in \mathbb{Z}$ such that $\theta_0 + \hat{\rho}(e, f) = \tilde{B}_e^f(\theta_0) = \theta_1 + m$.

Since $0 < \omega < \pi/2$, we have that $0 < F(\omega, e) < K(e)$. Then (31) implies $0 < \theta_1 - \theta_0 < \frac{1}{2}$. We conclude that

$$-\frac{1}{2} < m = \hat{\rho}(e, f) - (\theta_1 - \theta_0) = \hat{\rho}(e, f) - \frac{F(\omega, e)}{2K(e)} < 1.$$

Thus the integer $m = 0$ and this directly gives (4). \square

Remark 2. The geometric idea of the proof above is to choose two points $z_0, z_1 \in E(f)$ that are related by symmetry and that have the same value of the canonical momentum r_0 . The implication is that the line $\overrightarrow{z_0 z_1}$ is horizontal. Choosing φ_0, φ_1 as in (30), we define $z_0 = \gamma(\varphi_0)$ and $z_1 = \gamma(\varphi_1)$.

This implies that

$$z_0 = \frac{1}{f}(\sin \omega, \sqrt{1 - f^2} \cos \omega), \quad z_1 = \frac{1}{f}(-\sin \omega, \sqrt{1 - f^2} \cos \omega).$$

A simple computation from (4) shows that $(\sqrt{1 - f^2}/f) \cos \omega = \sqrt{1 - e^2}/e$. We conclude that the segment $\overrightarrow{z_0 z_1}$ is tangent to $E(e)$ at the point $(0, \frac{1}{e}\sqrt{1 - e^2})$, implying that $E(e)$ is a caustic for the orbit.

Remark 3. Some of the level sets of the rotation number (4) were shown in Fig. 2. Note that the curves in Fig. 2 begin at $(0, 0)$ and grow monotonically, ending at $(1, 1)$. The bounding values follow from two simple limits corresponding to the degenerate cases:

$$\lim_{f \rightarrow e^-} \hat{\rho}(e, f) = \lim_{e \rightarrow f^+} \hat{\rho}(e, f) = 0, \quad \lim_{f \rightarrow 0^+} \hat{\rho}(e, f) = \lim_{e \rightarrow 1^-} \hat{\rho}(e, f) = \frac{1}{2}.$$

The last limit is not trivial—it is shown in App. B. In §3.2, and in particular in Lem. 10, we will give an explicit formula that will explain the monotonicity. In App. C, we prove that (4) satisfies $\frac{\partial \hat{\rho}}{\partial e} > 0$ and $\frac{\partial \hat{\rho}}{\partial f} < 0$, see Lem. 31.

Using the formula (4) and geometrical considerations, one can find polynomial relations between the eccentricities e and f that correspond to low-order rational rotation numbers. It is generally difficult, however, to construct such polynomial relations for these level sets. In the next section we develop a general method to establish the relation between e and f to obtain a given fixed rotation number.

3 Poristic Confocal Ellipses and Gauss symmetry

The problem of identifying pairs of ellipses for which the rotation number of a Poncelet map is rational is known as the problem of Poncelet porisms. In §3.1 we recall this definition and—for the the map B_e^f —recall some of the explicit polynomials in (e, f) that correspond to low-order rational values for $\hat{\rho}(e, f)$. Then in §3.2 we obtain a general formula for the eccentricity f of the outer ellipse so that the Poncelet map for a given inner ellipse has a specified rotation number. In §3.3 we use this formula to find a transformation of f that halves the rotation number. Finally in §3.4 we show that the billiard rotation number has a symmetry that we call *Gauss symmetry*.

3.1 Poristic Parameters

We denote the subset of (3) with a given rotation number ℓ by

$$\Delta_\ell = \{(e, f) \in \Delta : \hat{\rho}(e, f) = \ell\}. \tag{32}$$

Several such curves were shown in Fig. 2. The non-empty level sets of $\hat{\rho}^{-1}(\mathbb{Q})$ correspond to porisms:

Definition 1 (Poristic Ellipses). *A pair of confocal ellipses $E(e)$ and $E(f)$ with eccentricities $0 < f < e < 1$ is **poristic** if the rotation number (4) of the Poncelet map is rational. For each $q \in \mathbb{Q}$, Δ_q will be called a **poristic parameter set**.*

Thus it is clear that a poristic pair (e, f) will generate a closed polygon with vertices on the outer ellipse, i.e., that $(B_e^f)^m$ is the identity for some $m \in \mathbb{N}$. The first few poristic sets are given by the polynomials

$$\Delta_{1/3} = \{(e, f) \in \Delta : e^2 + 2ef^3 - 2ef - f^4 = 0\}, \tag{33}$$

$$\Delta_{1/4} = \{(e, f) \in \Delta : e^2 + f^4 - 2f^2 = 0\}, \tag{34}$$

$$\Delta_{1/6} = \{(e, f) \in \Delta : 4e^4 f^2 - 3e^4 - 6e^2 f^4 + 4e^2 f^2 + f^8 = 0\}. \tag{35}$$

We verify (34) below, and in App. A we verify the set (33) and find $\Delta_{1/5}$ and $\Delta_{2/5}$. The set (35) is obtained in §3.3.

Example 4 (Period Four Porism). To show that $\hat{\rho}(e, f) = \frac{1}{4}$ for (34), we substitute the polynomial into (4) to obtain

$$\hat{\omega}(e, f)|_{\Delta_{1/4}} = \arcsin\left(\frac{1}{\sqrt{2-f^2}}\right) = \arcsin\left(\frac{1}{\sqrt{1+e'}}\right),$$

with $e' := \sqrt{1-e^2}$. Then using [BF71, Form. 110.04]

$$F(\hat{\omega}(e, f), e) = \frac{1}{2}K(e), \quad (36)$$

we see that (4) implies that the rotation number is $\hat{\rho}(e, f) = \frac{1}{4}$.

It is interesting to contrast this with a direct computation of the orbit. If we let $z_0 = (x_0, y_0) = (1/e, -e'/e)$, $z_1 = (-x_0, y_0)$, $z_2 = (-x_0, -y_0)$, $z_3 = (x_0, -y_0)$, and $z_4 = z_0$, then (34) implies that $z_k \in E(f)$, where $E(f)$ is the outer ellipse given by (2). A direct computation shows that each directed segment $\overrightarrow{z_k z_{k+1}}$ is tangent to the ellipse $E(e)$, and has positive orientation. This implies that the circle map satisfies $B_e^f(z_k) = z_{k+1}$ so that $(B_e^f)^4 = id$ and $\hat{\rho}(e, f) = \frac{1}{4}$.

3.2 Explicit Porisms

More generally, we can obtain an explicit formula for the eccentricity f of the outer ellipse for a given caustic e and any given rotation number $\hat{\rho}(e, f) = \ell$.

Lemma 10 (Explicit porism). *If $(e, f) \in \Delta$, (3), and $\ell \in (0, 1/2)$, then $\hat{\rho}(e, f) = \ell$ if and only if*

$$f = e \operatorname{sn}(K(e)(2\ell + 1), e) = e \operatorname{cd}(2K(e)\ell, e). \quad (37)$$

Thus the map $e \mapsto (e, e \operatorname{cd}(2K(e)\ell, e))$, for $0 < e < 1$, parameterizes the curve Δ_ℓ .

Proof. We will show only one direction. The converse is similar. To compute $\hat{\omega}(e, f)$ using (4), note that (37) gives

$$\frac{e^2 - f^2}{e^2(1 - f^2)} = \frac{1 - \operatorname{cd}^2(u, e)}{1 - e^2 \operatorname{cd}^2(u, e)} = \operatorname{sn}^2(u, e),$$

where $u = 2K(e)\ell$. Given that $\ell \in (0, 1/2)$, then $0 < \operatorname{am}(2K(e)\ell, e) < \frac{\pi}{2}$, and (4) implies that $\hat{\omega}(e, f) = \arcsin(\operatorname{sn}(2K(e)\ell, e)) = \operatorname{am}(2K(e)\ell, e)$. This implies $F(\hat{\omega}(e, f), e) = 2K(e)\ell$, and the rotation number (4) becomes $\hat{\rho}(e, f) = \ell$. \square

An application of the Gauss transformation of elliptic integrals to the relation (37) is given in §3.4.

Remark 5. In Fig. 2, we observed that the set Δ is foliated by the curves Δ_ℓ , for $\ell \in (0, 1/2)$. In the figure, each Δ_ℓ is the graph of a function of e as in Lem. 10. Each of these curves appears to start at $(0, 0)$ and end at $(1, 1)$. This can be explained from (37) using the limits

$$\lim_{e \rightarrow 0^+} e \operatorname{cd}(2K(e)\ell, e) = 0, \quad \lim_{e \rightarrow 1^-} e \operatorname{cd}(2K(e)\ell, e) = 1,$$

that are valid for $\ell \in (0, 1/2)$. Since that $K(e) \rightarrow \infty$ when $e \rightarrow 1^-$, the second limit is non-trivial and requires appropriate asymptotic analysis, as we see in App. B. In addition, we can use Lem. 30 to show that $\frac{\partial f}{\partial \ell} < 0$ and $\frac{\partial f}{\partial e} > 0$. More details can be found in App. C.

3.3 Half-Rotation Number

The explicit poristic formula in Lemma 10 can be used with double-angle formulas for Jacobi elliptic functions to find a transformation of $(e, f) \in \Delta$ that will halve the rotation number.

Lemma 11 (Half-rotation). *Given $\ell \in (0, 1/2)$, $0 < e < 1$ and $f_0 = e \operatorname{cd}(2K(e)\ell, e)$, define*

$$f_1 = \sqrt{\frac{e(e+f_0)}{1+ef_0+s}}, \quad f_2 = \sqrt{\frac{e(e-f_0)}{1-ef_0+s}}, \quad s \equiv \sqrt{(1-e^2)(1-f_0^2)}. \quad (38)$$

Then $f_1 = e \operatorname{cd}(K(e)\ell, e)$, $f_2 = e \operatorname{cd}(K(e)(1-\ell), e)$, and

$$\hat{\rho}(e, f_1) = \frac{1}{2}\hat{\rho}(e, f_0), \quad \hat{\rho}(e, f_2) = \frac{1}{2} - \frac{1}{2}\hat{\rho}(e, f_0),$$

so that when $(e, f_0) \in \Delta_\ell$, then $(e, f_1) \in \Delta_{\ell/2}$, and $(e, f_2) \in \Delta_{1/2-\ell/2}$.

Proof. Using (37), the double angle formulas for Jacobi elliptic functions [BF71, Form.124.01] give

$$\frac{f_0}{e} = \operatorname{cd}(2K(e)\ell, e) = \frac{u-v}{1-e^2uv}, \quad (39)$$

where $u = \operatorname{cd}^2(K(e)\ell, e)$ and

$$v = \operatorname{sn}^2(K(e)\ell, e) = \frac{1 - \operatorname{cd}^2(K(e)\ell, e)}{1 - e^2 \operatorname{cd}^2(K(e)\ell, e)} = \frac{1-u}{1-e^2u}. \quad (40)$$

Using (39) and (40) we find that

$$\frac{f_0}{e} = \frac{-e^2u^2 + 2u - 1}{e^2u^2 - 2e^2u + 1} = \frac{e^2v^2 - 2v + 1}{e^2v^2 - 2e^2v + 1}, \quad (41)$$

which can be solved for u to give

$$u = \frac{1 + ef_0 - s}{e(e + f_0)} = \frac{e + f_0}{e(1 + ef_0 + s)}.$$

Since $\ell \in (0, 1/2)$, then $\operatorname{cd}(K(e)\ell, e) > 0$, so that by (38), $f_1 = e\sqrt{u} = e \operatorname{cd}(K(e)\ell, e)$.

Similarly, solving (41) for v , gives

$$v = \frac{1 - ef_0 - s}{e(e - f_0)} = \frac{e - f_0}{e(1 - ef_0 + s)}.$$

Since $\ell \in (0, 1/2)$, $\operatorname{sn}(K(e)\ell, e) > 0$, so that by (38), $f_2 = e\sqrt{v} = e \operatorname{sn}(K(e)\ell, e) = e \operatorname{cd}(K(e)(1-\ell), e)$. These results clearly imply that $0 < f_1, f_2 < e$ and hence $(e, f_1), (e, f_2) \in \Delta$. Finally, Lemma 10 implies that $\hat{\rho}(e, f_1) = \frac{1}{2}\hat{\rho}(e, f_0)$, and $\hat{\rho}(e, f_2) = \frac{1}{2} - \frac{1}{2}\hat{\rho}(e, f_0)$. \square

Example 6. An example of the application of Lem. 11 is shown in Fig. 6. Panel (a) shows a pair $E(e)$ and $E(f_0)$ with $(e, f_0) \in \Delta_{2/7}$. Using (38), gives a new outer ellipse in panel (b) with $\hat{\rho}(e, f_2) = \frac{1}{2} - \frac{1}{7} = \frac{5}{14}$.

Example 7. The half-rotation formula (38), in conjunction with (33) immediately gives (35).

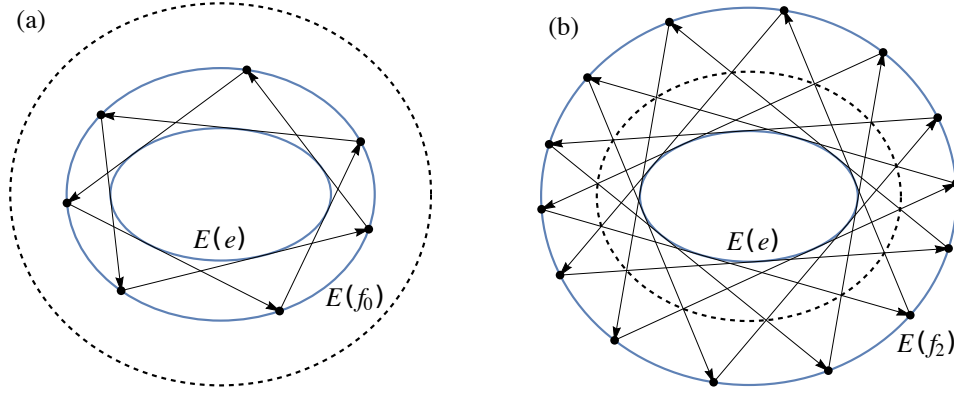


Figure 6: An example of the half-rotation formulas (38). (a) A pair of poristic ellipses $E(e), E(f_0)$ with $(e, f_0) = (0.8, 0.572851)$, and $\hat{\rho}(e, f_0) = 2/7$. (b) Mapping (e, f_0) to $(e, f_2) = (0.8, 0.419316)$, gives a pair $E(e), E(f_2)$ that is still poristic with $\hat{\rho}(e, f_2) = 5/14$. The dashed ellipses $E(f_2)$ in (a) and $E(f_0)$ in (b) are drawn for comparison.

3.4 Gauss Symmetry

In this section we obtain a symmetry for the rotation number (4) and show that any point (e, f) with a given rotation number can be transformed into an infinite number of such points with the same rotation number.

Landen and Gauss discovered some useful transformations of elliptic integrals which can be used to obtain a symmetry of the billiard rotation number. We will call this map *Gauss symmetry*.

Lemma 12 (Gauss symmetry). *Define the function $\mathfrak{g} : \mathbb{R}^+ \rightarrow (0, 1]$ by*

$$\mathfrak{g}(e) = \frac{2\sqrt{e}}{1+e}.$$

If $G : \Delta \rightarrow \Delta$ is the transformation

$$G(e, f) = (\mathfrak{g}(e), \mathfrak{g}(f^2 \cdot e^{-1})) = \left(\frac{2\sqrt{e}}{1+e}, \frac{2\sqrt{ef}}{f^2+e} \right), \quad (42)$$

then the rotation number $\hat{\rho}$ given by (4) is invariant under G ; i.e., $\hat{\rho} \circ G = \hat{\rho}$.

Proof. Fix eccentricities $0 < f < e < 1$. Using (4), we define $\omega_1 = \hat{\omega}(e, f)$ and $\omega_2 = \hat{\omega}(G(e, f))$. Clearly $0 < \omega_1, \omega_2 < \frac{\pi}{2}$, and a direct computation shows that

$$\sin(\omega_2)(1 + e \sin^2 \omega_1) = (1 + e) \sin \omega_1.$$

The Gauss transformation [GR65, Formula 8.125.3] of the elliptic integral (24) then implies that

$$F(\omega_2, \mathfrak{g}(e)) = \int_0^{\omega_2} \frac{d\tau}{\sqrt{1 - \mathfrak{g}(e)^2 \sin^2 \tau}} = (1 + e)F(\omega_1, e).$$

In particular, we note that $K(\mathfrak{g}(e)) = F(\frac{\pi}{2}, \mathfrak{g}(e)) = (1 + e)F(\frac{\pi}{2}, e) = (1 + e)K(e)$.

Using (4), we conclude that

$$\hat{\rho}(G(e, f)) = \frac{1}{2} \frac{F(\omega_2, \mathfrak{g}(e))}{K(\mathfrak{g}(e))} = \frac{1}{2} \frac{(1 + e)F(\omega_1, e)}{(1 + e)K(e)} = \hat{\rho}(e, f),$$

which is the promised result. □

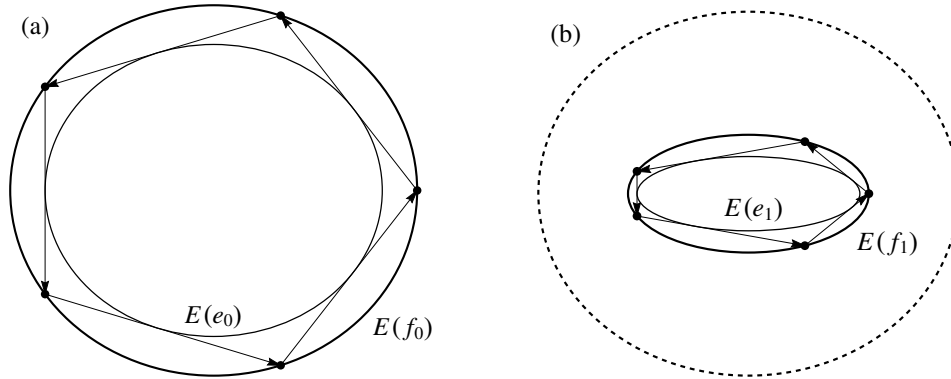


Figure 7: An example of Gauss symmetry with $\rho = \frac{1}{5}$. (a) A pair of ellipses $E(e_0), E(f_0)$ with $(e_0, f_0) = (0.6, 0.503246)$, and an orbit of the resulting Poncelet map. (b) Gauss symmetry transforms (e_0, f_0) to $(e_1, f_1) = G(e_0, f_0) = (0.968246, 0.913706)$, giving a pair $E(e_1), E(f_1)$ that still has $\hat{\rho}(e_1, f_1) = \frac{1}{5}$. The dashed ellipse is $E(f_0)$, drawn for comparison.

As a consequence of this Gauss symmetry, given $(e, f) \in \Delta$, the orbit of G gives an infinite number of points in Δ with the same rotation number. An example of the application of (42) is shown in Fig. 7. Panel (a) shows a pair of ellipses and an orbit for $\hat{\rho}(e_0, f_0) = \frac{1}{5}$. Under G , this transforms to eccentricities (e_1, f_1) , as shown in panel (b), with the same rotation number.

Note that an immediate consequence of Lem. 12 is the following.

Corollary 13. *The poristic set Δ_ℓ (32) is invariant under G : if $(e, f) \in \Delta_\ell$, then so is $G(e, f)$.*

In particular, if a polynomial expression—like that in (33)—defines a poristic parameter set, the polynomial must be invariant under the symmetry.

4 Pencils of Ellipses

To prepare for §5, where we will generalize the results of §2 for confocal ellipses to a Poncelet map between any pair of nested ellipses, we develop in this section some notation and coordinate transformations.

In §4.1 we recall the definition of a *pencil* as the family of linear combinations of the implicit equations for a pair of ellipses. For our analysis, we will fix the outer ellipse \mathcal{C}_o , and choose an element \mathcal{C}_ν of the pencil that is in its interior. We will show in §4.2 that there is a linear transformation of any pencil to a diagonal form that is characterized by three eigenvalues.

For each ν , the corresponding Poncelet map P_ν (9) is the map that uses $\mathcal{C}_i = \mathcal{C}_\nu$ as the interior ellipse. In §4.3 we obtain a key invariant that we call the *eccentricity of the pencil*. The dynamics of any of the Poncelet maps P_ν can be characterized in terms of Jacobi elliptic functions that have moduli give by this eccentricity. In §4.4, we will show that any pencil can be transformed, by a projective transformation, to a standard pencil for which the outer ellipse becomes the unit circle and the inner ellipse is centered at the origin with its principle axes aligned with the coordinate axes. This transformation can also be applied to the Poncelet map, giving a conjugate map.

4.1 Standing Assumptions

A conic \mathcal{C} in the plane can be represented by a real, 3×3 symmetric matrix C —using homogeneous coordinates—as the set (5). In order that \mathcal{C} be an ellipse we assume that the upper-left 2×2 minor of C is positive definite.² i.e., $\mathbf{w}^T C \mathbf{w} > 0$, whenever $\mathbf{w} = (x, y, 0)^T \neq \mathbf{0}$. That is, we will assume that the

²Of course, we could replace C by $-C$ to obtain these signs if necessary.

quadratic terms of (5) are positive definite. As a consequence, to have a nonempty \mathcal{C} , the full 3×3 matrix C must be indefinite, thus $\det C < 0$. We will refer to matrices with these properties as having the *ordered signature* $(+, +, -)$. In this case it is clear that the interior of the ellipse (5) is the set of points $(x, y) \in \mathbb{R}^2$ such that $\mathbf{u}^T C \mathbf{u} < 0$, where $\mathbf{u} = (x, y, 1)$.

If C_1 and C_2 are two symmetric matrices, with corresponding conics \mathcal{C}_1 and \mathcal{C}_2 , respectively, the associated pencil $\mathcal{C}_\nu = \mathcal{C}_{(\nu_1, \nu_2)}$ is the family (6) for $\nu = (\nu_1, \nu_2) \in \mathbb{R}^2$. The interior of \mathcal{C}_ν is

$$\text{Int}(\mathcal{C}_\nu) = \{(x, y) \in \mathbb{R}^2 : \mathbf{u}^T(\nu_1 C_1 + \nu_2 C_2)\mathbf{u} < 0, \mathbf{u} = (x, y, 1)^T\}.$$

An example is sketched in Fig. 8. Note that $\mathcal{C}_\nu = \mathcal{C}_\mu$ if the vectors ν and μ are non-zero and parallel, i.e., $\mathcal{C}_{\delta\nu} = \{\delta\mathbf{u}^T(\nu_1 C_1 + \nu_2 C_2)\mathbf{u} = 0\} = \mathcal{C}_\nu$, for any $\delta \neq 0$. Thus the pencil is defined on the projective line $\nu \in \mathbb{P}^1$. We will restrict to parameters for which $\mathcal{C}_\nu \subset \text{Int}(\mathcal{C}_1)$.

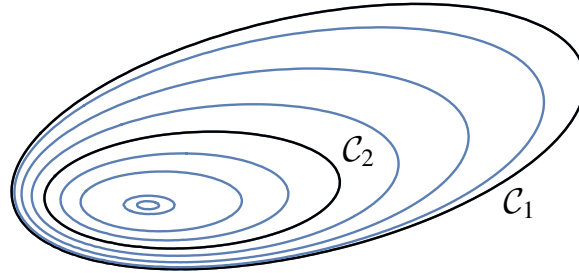


Figure 8: A pencil of ellipses generated by an outer ellipse \mathcal{C}_1 and an inner ellipse \mathcal{C}_2 . Each pair of ellipses of the pencil will generate a Poncelet map.

For the analysis below, we make the following assumptions on the matrices in the pencil (6):

(SA1) The symmetric 3×3 matrices C_1 and C_2 have ordered signature $(+, +, -)$: their upper-left 2×2 minors are positive definite, and $\det C_i < 0$. In particular,

$$(x, y, 0)C_i(x, y, 0)^T > 0, \quad \text{for all } (x, y) \neq (0, 0). \quad (43)$$

(SA2) The matrix $C_1^{-1}C_2$ has three positive, distinct eigenvalues.

(SA3) The ellipse \mathcal{C}_2 is inside \mathcal{C}_1 ; that is, whenever $\mathbf{u} \neq 0$ and $\mathbf{u}^T C_2 \mathbf{u} = 0$, then $\mathbf{u}^T C_1 \mathbf{u} < 0$.

Remark 8. The concept of *generalized eigenvalues of a pencil*, discussed in [Par98, SS90] is related to our construction. Given a pair of matrices C_1, C_2 , the generalized eigenvalues of the pencil generated by (C_1, C_2) , are the roots of the polynomial $\det(\lambda C_1 - C_2)$. Since (SA1) implies that C_1 is invertible, the eigenvalues mentioned in (SA2) are the generalized eigenvalues of the pencil.

Remark 9. Standing assumption (SA3) follows because by (43), whenever $\mathbf{u} = (x, y, z)$ and $\mathbf{u}^T C_2 \mathbf{u} = 0$, we must have $z \neq 0$. Thus on the ellipse (5), we can scale the vector $(x, y, 1)^T$ by z to obtain $\mathbf{u}^T C_2 \mathbf{u} = 0$ for the more general vector $\mathbf{u} = (zx, zy, z)^T$. Similarly when $(x, y, 1)C_1(x, y, 1)^T < 0$, the corresponding scaled equation $\mathbf{u}^T C_1 \mathbf{u} < 0$ as well since each term in the quadratic form is scaled by $z^2 > 0$.

Remark 10. There is some freedom in the choice of matrices to represent the ellipses. For example, if the pair (C_1, C_2) satisfies the assumptions, then whenever $\delta, \gamma > 0$, the pair $(\delta C_1, \gamma C_2)$ does as well. Indeed, the eigenvalues of Asm. (SA2) are homogeneous of degree one in C_1 , and homogeneous of degree minus one in C_2 .

4.2 Simultaneous Diagonalization

Here we will show that there is a transformation of the pair of matrices that satisfy the assumptions of §4.1 to diagonal form.

Lemma 14. *If the matrices C_1, C_2 obey Asm. (SA1)-(SA3) then there exists a nonsingular matrix M such that*

$$M^T C_1 M = \text{diag}(1, 1, -1), \quad \text{and} \quad M^T C_2 M = \text{diag}(\lambda_1, \lambda_2, -\lambda_3), \quad (44)$$

where $\{\lambda_1, \lambda_2, \lambda_3\}$ are the eigenvalues of $C_1^{-1}C_2$, and

$$\lambda_1 > \lambda_2 > \lambda_3 > 0. \quad (45)$$

Proof. To obtain (44), Asm. (SA2) implies there exists an invertible matrix Q_0 that diagonalizes $C_1^{-1}C_2$; that is

$$Q_0^{-1}C_1^{-1}C_2Q_0 = D,$$

where D is diagonal and positive definite. This clearly implies that $Q_0^T C_2 Q_0 = (Q_0^T C_1 Q_0)D$. Noting that $Q_0^T C_2 Q_0$ and $Q_0^T C_1 Q_0$ are symmetric, then the commutator $[Q_0^T C_1 Q_0, D] = 0$. Since the entries of D are assumed distinct, then $Q_0^T C_1 Q_0$ must be diagonal. Finally $Q_0^T C_2 Q_0$ is the product of diagonal matrices, so it too is diagonal.

Recall that Sylvester's law of inertia implies that the signature does not change under a congruency. Thus by Asm. (SA1) there are exactly two positive and one negative entries on the diagonals of the congruent matrices $Q_0^T C_1 Q_0$ and $Q_0^T C_2 Q_0$, and the negative entry is in the same position in both, since D is positive definite. With an appropriate elementary permutation matrix Q_1 , we can swap a pair of rows and the same pair of columns to order these entries, i.e.,

$$Q_1^T (Q_0^T C_1 Q_0) Q_1 = \text{diag}(\alpha_1, \alpha_2, \alpha_3),$$

where $\alpha_1, \alpha_2 > 0$, and $\alpha_3 < 0$. If we let $T = \text{diag}\left(\frac{1}{\sqrt{\alpha_1}}, \frac{1}{\sqrt{\alpha_2}}, \frac{1}{\sqrt{-\alpha_3}}\right)$ and $M = Q_0 Q_1 T$, then

$$M^T C_1 M = T^T Q_1^T Q_0^T C_1 Q_0 Q_1 T = T \text{diag}(\alpha_1, \alpha_2, \alpha_3) T = \text{diag}(1, 1, -1),$$

giving the form (44). Finally, since $C_2 = C_1 Q_0 D Q_0^{-1}$, a simple computation then gives

$$\begin{aligned} M^T C_2 M &= M^T C_1 Q_0 D Q_0^{-1} Q_0 Q_1 T = M^T C_1 M M^{-1} Q_0 D Q_1 T \\ &= \text{diag}(1, 1, -1) T^{-1} (Q_1^T D Q_1) T, \end{aligned}$$

where, since Q_1 is an elementary permutation, $Q_1^{-1} = Q_1^T$. Now defining the reordered eigenvalues so that $T^{-1} Q_1^T D Q_1 T = \text{diag}(\lambda_1, \lambda_2, \lambda_3)$, gives

$$M^T C_2 M = \text{diag}(1, 1, -1) \text{diag}(\lambda_1, \lambda_2, \lambda_3),$$

which is equivalent to (44). Clearly, $\{\lambda_1, \lambda_2, \lambda_3\}$ are the eigenvalues of $C_1^{-1}C_2$.

It remains to show that the ordering (45) holds. Suppose that $(w_1, w_2) \neq (0, 0)$ are arbitrary and

$$\mathbf{w} = (w_1, w_2, w_3) = \left(w_1, w_2, \sqrt{\frac{\lambda_1 w_1^2 + \lambda_2 w_2^2}{\lambda_3}} \right).$$

If $\mathbf{u} = M\mathbf{w}$, then both \mathbf{w} and \mathbf{u} are non-zero and (5) implies that

$$\mathbf{u}^T C_2 \mathbf{u} = \mathbf{w}^T M^T C_2 M \mathbf{w} = \lambda_1 w_1^2 + \lambda_2 w_2^2 - \lambda_3 w_3^2 = 0,$$

so that \mathbf{u} is a point on \mathcal{C}_2 . By Asm. (SA3), \mathcal{C}_2 is in the interior of \mathcal{C}_1 ; therefore we must have $\mathbf{u}^T C_1 \mathbf{u} < 0$. Using the definitions of \mathbf{u} and \mathbf{w} , this inequality transforms to

$$\mathbf{u}^T C_1 \mathbf{u}^T = \mathbf{w}^T M^T C_1 M \mathbf{w} = w_1^2 + w_2^2 - w_3^2 = \left(1 - \frac{\lambda_1}{\lambda_3}\right) w_1^2 + \left(1 - \frac{\lambda_2}{\lambda_3}\right) w_2^2 < 0.$$

Since this must be true for any $(w_1, w_2) \neq (0, 0)$, we must have $\lambda_3 < \lambda_2, \lambda_1$. Without loss of generality we can assume that $\lambda_2 < \lambda_1$, since by Asm. (SA2) the eigenvalues are distinct; indeed this ordering can be obtained by changing the permutation matrix Q_1 if needed. This concludes the proof. \square

Remark 11. The previous lemma can be regarded as a simultaneous diagonalization result in the context of generalized eigenvalues. Similar results about the diagonalization—and the order of the eigenvalues—are known [Par98, SS90] for the case in which one of the matrices is positive definite. In our case the positive definite condition is replaced by Asm. (SA1)-(SA3).

Given the normal forms (44), we next obtain conditions on the parameters (ν_1, ν_2) , so that members of the family (6) also satisfy the standing assumptions.

Lemma 15. *Suppose that C_1 and C_2 satisfies Asm. (SA1)-(SA3), and that $\boldsymbol{\nu} = (\nu_1, \nu_2)$ satisfy (7), e.g., $\nu_2 > 0$ and $\nu_1 + \lambda_3 \nu_2 > 0$. Then the pair of matrices $(C_1, C_{\boldsymbol{\nu}})$, with $C_{\boldsymbol{\nu}} = \nu_1 C_1 + \nu_2 C_2$, also satisfies the standing assumptions. In this case, we say that $\boldsymbol{\nu} = (\nu_1, \nu_2)$ is a valid parameter vector.*

Proof. Using Lem. 14, there is a matrix M giving (44) where $\lambda_1 > \lambda_2 > \lambda_3 > 0$. This implies that

$$C_2 - \lambda_3 C_1 = M^{-T} \text{diag}(\lambda_1 - \lambda_3, \lambda_2 - \lambda_3, 0) M^{-1}.$$

Since both $\lambda_1 - \lambda_3$ and $\lambda_2 - \lambda_3 > 0$, the matrix $C_2 - \lambda_3 C_1$ is positive semi-definite. Thus $\mathbf{u}^T (C_2 - \lambda_3 C_1) \mathbf{u} \geq 0$, for all $\mathbf{u} \in \mathbb{R}^3$. We can write the matrix $C_{\boldsymbol{\nu}}$ of (6) as

$$C_{\boldsymbol{\nu}} = \nu_1 C_1 + \nu_2 C_2 = (\nu_1 + \lambda_3 \nu_2) C_1 + \nu_2 (C_2 - \lambda_3 C_1).$$

Note that when $\boldsymbol{\nu}$ satisfies the restrictions (7) then since $C_2 - \lambda_3 C_1$ is positive semi-definite, and C_1 satisfies Asm. (SA1), then $C_{\boldsymbol{\nu}}$ must have a positive definite upper-left minor. That is, $(x, y, 0) C_{\boldsymbol{\nu}} (x, y, 0)^T > 0$ whenever $(x, y) \neq (0, 0)$. This proves that $C_{\boldsymbol{\nu}}$ satisfies Asm. (SA1).

To verify Asm. (SA2), it is enough to notice that the eigenvalues of $C_1^{-1} C_{\boldsymbol{\nu}}$ are $\{\tilde{\lambda}_1, \tilde{\lambda}_2, \tilde{\lambda}_3\}$, where $\tilde{\lambda}_i = \nu_1 + \lambda_i \nu_2$. Then (45) and (7) imply that $0 < \tilde{\lambda}_3 < \tilde{\lambda}_2 < \tilde{\lambda}_1$. This proves Asm. (SA2).

Finally, to prove Asm. (SA3), assume that $\mathbf{u} \neq \mathbf{0}$ satisfies $\mathbf{u}^T C_{\boldsymbol{\nu}} \mathbf{u} = 0$. We want to show that $\mathbf{u}^T C_1 \mathbf{u} < 0$. Since $C_2 - \lambda_3 C_1$ is positive semi-definite,

$$(\nu_1 + \lambda_3 \nu_2) \mathbf{u}^T C_1 \mathbf{u} = \mathbf{u}^T (-\nu_2 C_2 + \lambda_3 \nu_2 C_1) \mathbf{u} = -\nu_2 \mathbf{u}^T (C_2 - \lambda_3 C_1) \mathbf{u} \leq 0.$$

If it were the case that $\mathbf{u}^T C_1 \mathbf{u} = 0$, then the above inequality implies that $\mathbf{u}^T C_2 \mathbf{u} = 0$. However, then Asm. (SA3) would imply that $\mathbf{u}^T C_1 \mathbf{u} < 0$. This is a contradiction, so the only possibility is that $\mathbf{u}^T C_1 \mathbf{u} < 0$, and this implies Asm. (SA3). \square

The region defined in (7) is sketched in Fig. 9. Note that it is the cone generated by the two extreme cases $\mathcal{C}_o = \mathcal{C}_1$ and \mathcal{C}_∞ that correspond to the vectors and $(1, 0)$ and $(-\lambda_3, 1)$, respectively (see §4.4 below). Moreover, by Lem. 15, $\mathcal{C}_{\boldsymbol{\nu}} \subset \text{Int}(\mathcal{C}_1)$, whenever $\boldsymbol{\nu} = (\nu_1, \nu_2)$ is in this region.

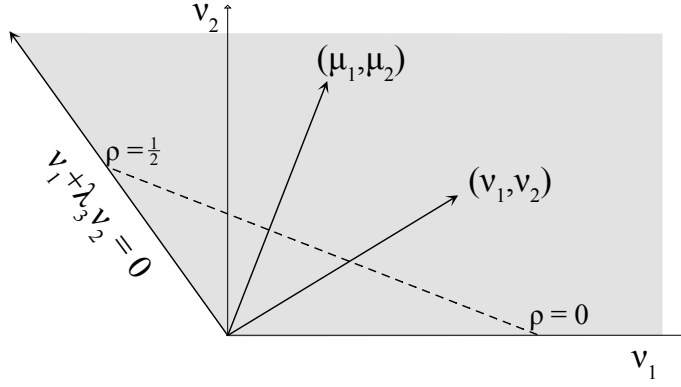


Figure 9: Shaded region of the parameter plane (ν_1, ν_2) in which the pencil (6) obeys conditions (7) so that C_ν is inside C_1 . The representative vectors correspond to C_μ being inside C_ν according to Lem. 15. The dashed line shows the variation of the rotation number along the segment (61).

4.3 Pencil Eccentricity

For a pair of ellipses satisfying the standing assumptions, the *pencil eccentricity* (8) is an invariant that depends only on the eigenvalues $\lambda_1, \lambda_2, \lambda_3$ of $C_1^{-1}C_2$. As we will see below, this quantity determines the rotation number of the associated Poncelet map. First we show that the eccentricity is pencil invariant: given an outer ellipse the eccentricity is the same for *any* interior ellipse of the pencil.

Lemma 16. *Suppose that C_1 and C_2 satisfy Asm. (SA1)-(SA3) and that C_ν is the associated pencil (6). Then if ν and μ satisfy (7), the eccentricity of the pencil is invariant:*

$$e(C_1, C_\nu) = e(C_1, C_\mu) = e(C_1, C_2).$$

More generally, if C_μ is inside C_ν , then

$$e(C_\nu, C_\mu) = \sqrt{\frac{\nu_1 + \lambda_3 \nu_2}{\nu_1 + \lambda_2 \nu_2}} e(C_1, C_2). \quad (46)$$

Proof. The eigenvalues of $C_1^{-1}C_\nu$ are precisely $\tilde{\lambda}_i = \nu_1 + \lambda_i \nu_2$, $i = 1, 2, 3$. This implies that

$$e(C_1, C_\nu) = \sqrt{\frac{\tilde{\lambda}_1 - \tilde{\lambda}_2}{\tilde{\lambda}_1 - \tilde{\lambda}_3}} = \sqrt{\frac{\lambda_1 - \lambda_2}{\lambda_1 - \lambda_3}} = e(C_1, C_2).$$

For the more general case, note that the eigenvalues of the matrix $C_\nu^{-1}C_\mu$ are

$$\bar{\lambda}_i = \frac{\mu_1 + \lambda_i \mu_2}{\nu_1 + \lambda_i \nu_2},$$

thus

$$e(C_\nu, C_\mu) = \sqrt{\frac{\bar{\lambda}_1 - \bar{\lambda}_2}{\bar{\lambda}_1 - \bar{\lambda}_3}} = \sqrt{\frac{\nu_1 + \lambda_3 \nu_2}{\nu_1 + \lambda_2 \nu_2}} \sqrt{\frac{(\nu_1 \mu_2 - \nu_2 \mu_1)(\lambda_1 - \lambda_2)}{(\nu_1 \mu_2 - \nu_2 \mu_1)(\lambda_1 - \lambda_3)}},$$

which reduces to the promised expression (46). \square

Remark 12. Note that, as in Rem. 10, the eccentricity (8) is also invariant under the scaling transformation: $e(C_1, C_2) = e(\delta C_1, \gamma C_2)$, for $\delta, \gamma > 0$. Furthermore, whenever C_1 and C_2 satisfy Asm. (SA2), then so do the pair of congruent matrices $\tilde{C}_1 = S^T C_1 S$ and $\tilde{C}_2 = S^T C_2 S$, when S is invertible. Note that, since $\tilde{C}_1^{-1} \tilde{C}_2 = S^{-1} (C_1^{-1} C_2) S$, the eigenvalues for Asm. (SA2) are unchanged. Thus, the eccentricity is invariant under such a transformation: $e(C_1, C_2) = e(\tilde{C}_1, \tilde{C}_2)$.

4.4 Projective Transformations

In this section we will use the matrix M that satisfies (44) to create a projective transformation of the plane. Recall that under a projective transformation, lines are transformed into lines, and quadrics into quadrics. Thus such a transformation preserves collinearity and tangency between two curves. For application to Poncelet maps, we will also require that the projective transformation be an orientation preserving diffeomorphism.

Definition 2 (Standard Projective Transformation). *A 3×3 matrix M defines a map of the plane*

$$\widehat{M} \begin{pmatrix} x \\ y \end{pmatrix} = \begin{pmatrix} \frac{m_{11}x + m_{12}y + m_{13}}{m_{31}x + m_{32}y + m_{33}} \\ \frac{m_{21}x + m_{22}y + m_{23}}{m_{31}x + m_{32}y + m_{33}} \end{pmatrix}. \quad (47)$$

Lemma 17. *If M is a matrix giving (44), then $\widehat{M} : \mathbb{D} \rightarrow \widehat{M}(\mathbb{D})$ is a diffeomorphism, where \mathbb{D} is the unit disk*

$$\mathbb{D} = \{(x, y) \in \mathbb{R}^2 : x^2 + y^2 \leq 1\}. \quad (48)$$

Proof. First we show that whenever $(x, y) \in \mathbb{D}$,

$$m_{31}x + m_{32}y + m_{33} \neq 0.$$

By way of contradiction, suppose that there exists a point $(x, y) \in \mathbb{D}$ and $u, v \in \mathbb{R}$, such that $M(x, y, 1)^T = (u, v, 0)^T$. Since M is nonsingular, $(u, v) \neq (0, 0)$, and thus $(u, v, 0)C_1(u, v, 0)^T > 0$ by Asm. (SA1). Using (44), we find that

$$x^2 + y^2 - 1 = (x, y, 1)M^T C_1 M(x, y, 1)^T = (u, v, 0)C_1(u, v, 0)^T > 0,$$

contradicting $(x, y) \in \mathbb{D}$. This gives the result. Finally, it is easy to see that \widehat{M} is one-to-one. Indeed, the inverse of the transformation (47) is simply obtained by replacing the nonsingular matrix M by its inverse. \square

Lemma 18. *The map (47) is orientation-preserving if and only if $\det(M) m_{33} > 0$.*

Proof. By Lem. 17 the denominator $m_{31}x + m_{32}y + m_{33} \neq 0$, for all $(x, y) \in \mathbb{D}$. In particular, $m_{33} \neq 0$ and $m_{31}x + m_{32}y + m_{33}$ does not change sign on \mathbb{D} . The determinant of the Jacobian of \widehat{M} is

$$\det \left(D\widehat{M}(x, y) \right) = \frac{\det(M)}{(m_{31}x + m_{32}y + m_{33})^3}.$$

Since the sign of the denominator above is the sign of m_{33} , we conclude that $\det \left(D\widehat{M}(x, y) \right) > 0$, for all $(x, y) \in \mathbb{D}$, if and only if $\det(M)$ and m_{33} have the same sign. \square

Remark 13. The matrix M defined by conditions (44) is not unique. If M satisfies (44), then any of the eight matrices,

$$M \operatorname{diag}(\pm 1, \pm 1, \pm 1),$$

will also satisfy equations (44). Hence, we can modify the matrix M and assume—without loss of generality—that $\det(M) m_{33} > 0$, so that \widehat{M} is orientation-preserving.

The projective transformation (47) can be applied to any pencil (6) under the restrictions (7) to give the simple form.

$$\bar{\mathcal{C}}_\nu \equiv \widehat{M}^{-1}(\mathcal{C}_\nu) = \{(X, Y) \in \mathbb{R}^2 : (\nu_1 + \lambda_1\nu_2)X^2 + (\nu_1 + \lambda_2\nu_2)Y^2 = \nu_1 + \lambda_3\nu_2\}. \quad (49)$$

Since \widehat{M} is an orientation preserving diffeomorphism, the interior of $\bar{\mathcal{C}}_\nu$ becomes

$$\text{Int}(\bar{\mathcal{C}}_\nu) = \widehat{M}^{-1}(\text{Int}(\mathcal{C}_\nu)) = \{(X, Y) \in \mathbb{R}^2 : (\nu_1 + \lambda_1\nu_2)X^2 + (\nu_1 + \lambda_2\nu_2)Y^2 < \nu_1 + \lambda_3\nu_2\}.$$

Note that in these coordinates the outer ellipse, where $\nu_2 = 0$, simply becomes the unit circle

$$\mathbb{S}^1 = \widehat{M}^{-1}(\mathcal{C}_{(1,0)}) = \{(X, Y) \in \mathbb{R}^2 : X^2 + Y^2 = 1\}.$$

and the inner ellipse, where $\nu_1 = 0$, becomes

$$\bar{\mathcal{C}}_i = \widehat{M}^{-1}(\mathcal{C}_{(0,1)}) = \{(X, Y) \in \mathbb{R}^2 : \lambda_1X^2 + \lambda_2Y^2 = \lambda_3\}. \quad (50)$$

The pencil (49) also contains the limiting ellipse, on the boundary $\nu_1 + \lambda_3\nu_2 = 0$ of the region (7). Choosing $\nu = (-\lambda_3, 1)$ to represent this case, then the corresponding transformed conic is simply the origin:

$$\bar{\mathcal{C}}_{(-\lambda_3,1)} = \{(0, 0)\}.$$

Of course this point is in the interior of all the ellipses in the pencil $\bar{\mathcal{C}}_\nu$. As a consequence, the limiting point for the pencil satisfies

$$\mathcal{C}_\infty \equiv \mathcal{C}_{(-\lambda_3,1)} = \{\widehat{M}(0, 0)\}. \quad (51)$$

Finally, under the assumption of Lem. 18, the Poncelet map $P : \mathcal{C}_o \rightarrow \mathcal{C}_o$, with respect to the interior ellipse \mathcal{C}_i , is transformed, by the conjugacy

$$\bar{P} = \widehat{M}^{-1} \circ P \circ \widehat{M}.$$

to a Poncelet map $\bar{P} : \mathbb{S}^1 \rightarrow \mathbb{S}^1$ with respect to the inner ellipse (50).

5 Poncelet maps for Pencils

In §5.1 we will show that the general pencil (6), with eccentricity e given by (8), can be mapped onto a *standard pencil* that we call \mathcal{S}_e^f so that the outermost ellipse is the unit circle. We see in §5.2 that this transformation conjugates (9) to the standard Poncelet map $P_e^f : \mathbb{S}^1 \rightarrow \mathbb{S}^1$ for the standard pencil. We will then find a second conjugacy that maps any pair of confocal ellipses (2) onto the standard pencil. The implication is that the billiard map B_e^f is also conjugate to P_e^f . Thus by this two-step process, we find a conjugacy between B_e^f and P_ν . An implication is that the rotation numbers of B_e^f , P_e^f , and P_ν are all equal to $\hat{\rho}(e, f)$.

In §5.3 we obtain the relation (10) between ν and the rotation number of the Poncelet map. We then prove Thm. 4, giving the inverse of this relation. Finally in §5.4, we prove that the rotation number satisfies the monotonicity condition Thm. 3.

5.1 Standard Pencil

A *standard pencil* is a family of ellipses with a common center for which the outermost is a circle:

Definition 3 (Standard Pencil). *The standard pencil with eccentricity $e \in (0, 1)$ is the one-parameter family of ellipses*

$$\mathcal{S}_e^f = \left\{ (X, Y) \in \mathbb{R}^2 : \left(\frac{1-f^2}{1-e^2} \right) X^2 + Y^2 = \frac{f^2}{e^2} \right\}, \quad (52)$$

for $0 \leq f \leq e$. The outermost conic $\mathcal{S}_e^e = \mathbb{S}^1$ is the unit circle, and the innermost is the limiting point $\mathcal{S}_e^0 = \{(0, 0)\}$.

Note that the ellipses in the set (52) are nested: whenever $f_1 < f_2$ then $\mathcal{S}_e^{f_1} \subset \text{Int}(\mathcal{S}_e^{f_2})$. Moreover, $\bigcup_{f=0}^e \mathcal{S}_e^f = \mathbb{D}$, the unit disk (48).

It is easy to see that $\{\mathcal{S}_e^f\}_{0 \leq f \leq e}$ is a pencil of the form (6). For the outer circle the associated matrix is $C_1 = \text{diag}(1, 1, -1)$ and for the ellipse \mathcal{S}_e^f , it is $C_2 = \text{diag}(\lambda_1 \lambda_2, -\lambda_3)$ where

$$\lambda_1 = \frac{1-f^2}{1-e^2}, \quad \lambda_2 = 1, \quad \lambda_3 = \frac{f^2}{e^2}. \quad (53)$$

Since these matrices are already diagonal, (53) are the eigenvalues for (44), and when $0 < f < e$, they satisfy the ordering (45). Using (8), the eccentricity of this pencil is therefore $e(C_1, C_2) = e$, which is—as expected—independent of f .

With some algebra, one can show that the standard Poncelet map, $P_e^f : \mathbb{S}^1 \rightarrow \mathbb{S}^1$, with respect to the inner ellipse \mathcal{S}_e^f , is explicitly

$$P_e^f(X, Y) = \left(-\frac{A_1 A_4 Y \sqrt{1-e^2 Y^2} + A_2 A_3 X}{A_2^2 - A_1^2 e^2 Y^2}, \frac{A_1 A_2 X \sqrt{1-e^2 Y^2} - A_3 A_4 Y}{A_2^2 - A_1^2 e^2 Y^2} \right), \quad (54)$$

where

$$\begin{aligned} A_1 &= 2f \sqrt{(1-f^2)(e^2-f^2)}, \\ A_2 &= e^2 - f^4, \\ A_3 &= e^2 + f^4 - 2f^2, \\ A_4 &= e^2(1-2f^2) + f^4. \end{aligned}$$

Note that when $f = 0$, $P_e^0(x, y) = (-x, -y)$, so that the segment $\overrightarrow{(x, y)P_e^0(x, y)}$ passes through the limiting point, \mathcal{S}_e^0 , so that the rotation number is $\frac{1}{2}$. Moreover, $P_e^e(x, y) = (x, y)$ is the identity map since $\mathcal{S}_e^e = \mathbb{S}^1$. As we will see, P_e^f is conjugate to B_e^f , so it has rotation number $\hat{\rho}(e, f)$.

The standard pencil (52) is mapped onto the general pencil using the transformation \widehat{M} of (47). Moreover a simple linear transformation maps the family of confocal ellipses (2) onto the standard pencil:

Lemma 19. *Given matrices C_1 and C_2 with eigenvalues $\lambda_1, \lambda_2, \lambda_3$ obeying *Asm.* (SA1)-(SA3), let \mathcal{C}_ν be the pencil (6) for a valid parameter vector $\nu = (\nu_1, \nu_2)$, satisfying (7). If $e = e(C_1, C_2)$ is the pencil eccentricity and*

$$f = f(\nu) = e \sqrt{\frac{\nu_1 + \lambda_3 \nu_2}{\nu_1 + \lambda_2 \nu_2}}, \quad (55)$$

then:

1) $\widehat{M}(\mathbb{S}^1) = \mathcal{C}_1$ and $\widehat{M}(\mathcal{S}_e^f) = \mathcal{C}_\nu$ using the transformation (47);

2) The linear transformation

$$T_f(x, y) = \left(\frac{f}{\sqrt{1-f^2}} y, -f x \right), \quad (56)$$

maps $T_f(E(f)) = \mathbb{S}^1$ and $T_f(E(e)) = \mathcal{S}_e^f$, where $E(\varepsilon)$ is the confocal family defined in (2).

Proof. By construction, the projective transformation \widehat{M} satisfies (49), which implies that $\widehat{M}^{-1}(\mathcal{C}_1) = \mathbb{S}^1$ since $\nu = (1, 0)$. Therefore, to prove the first part, it is enough to show that $\mathcal{S}_e^f = \widehat{M}^{-1}(\mathcal{C}_\nu)$. From (8) and (55), since $0 < f < e$, we find that

$$\frac{1-f^2}{1-e^2} = 1 + \left(\frac{e^2}{1-e^2} \right) \left(1 - \frac{f^2}{e^2} \right) = 1 + \left(\frac{\lambda_1 - \lambda_2}{\lambda_2 - \lambda_3} \right) \left(\frac{(\lambda_2 - \lambda_3)\nu_2}{\nu_1 + \lambda_2\nu_2} \right) = \frac{\nu_1 + \lambda_1\nu_2}{\nu_1 + \lambda_2\nu_2}.$$

This implies that \mathcal{S}_e^f has the same form as (49).

For the second part, given any point $(x, y) \in \mathbb{R}^2$, let $(X, Y) = T_f(x, y)$. A direct computation shows that $(x, y) \in E(f)$ if and only if $X^2 + Y^2 = 1$, and $(x, y) \in E(e)$ if and only if $(X, Y) \in \mathcal{S}_e^f$. \square

Remark 14. We know that the eccentricity of a pencil is invariant under projective transformations. In fact, as a consequence of Lem. 19, any pencil with eccentricity e is projectively-equivalent to the standard pencil $\{\mathcal{S}_e^f\}_{0 \leq f \leq e}$. Furthermore, two pencils of nested ellipses are projectively-equivalent if and only if they have the same eccentricity.

Remark 15. Suppose that $0 < f < e < 1$ and $\ell = \hat{\rho}(e, f)$. Substituting $f = e \operatorname{cd}(2K(e)\ell, e)$ from (37) into (52), implies that

$$\mathcal{S}_e^f = \{(X, Y) \in \mathbb{R}^2 : X^2 + \operatorname{dn}^2(2K(e)\ell, e) Y^2 = \operatorname{cn}^2(2K(e)\ell, e)\}.$$

This also implies that for a fixed pencil eccentricity e , the rotation number ℓ can be used to parameterize the standard pencil.

5.2 Standard Covering Space

Using Lem. 14 and Lem. 19, we will now obtain a general covering space that will simultaneously reduce all Poncelet maps, and make them conjugate to rigid rotation.

Definition 4 (Standard Covering Map). *Let C_1 and C_2 be a pair of matrices obeying Asm. (SA1)-(SA3). If M diagonalizes C_1 and C_2 as in (44), and $\det(M)m_{33} > 0$, then the standard covering map $\Pi_M : \mathbb{R} \rightarrow \mathcal{C}_1$, is*

$$\Pi_M(\theta) = \widehat{M} \begin{pmatrix} \operatorname{cn}(4K(e)\theta, e) \\ \operatorname{sn}(4K(e)\theta, e) \end{pmatrix}, \quad (57)$$

where \widehat{M} is given in (47) and e is the pencil eccentricity (8).

Remark 16. The parameterization (57) is well defined since Lem. 17 implies that the denominator in these terms can never be zero because $(\operatorname{sn}(u, e), \operatorname{cn}(u, e)) \in \mathbb{D}$. Moreover, the periodicity of the Jacobi elliptic functions implies that Π_M is a covering map with group of deck transformations generated by $\theta \mapsto \theta + 1$. The condition $\det(M)m_{33} > 0$ is important so that \widehat{M} is orientation-preserving. In particular, if M is the identity, then $\theta \mapsto (\operatorname{cn}(4K(e)\theta, e), \operatorname{sn}(4K(e)\theta, e))$ is the covering map for the standard pencil.

Lemma 20. *Suppose that \mathcal{C}_ν is a pencil (6) with eigenvalues $\lambda_1 > \lambda_2 > \lambda_3 > 0$ and pencil eccentricity e . If $P_\nu : \mathcal{C}_1 \rightarrow \mathcal{C}_1$ is the family of Poncelet circle maps for the pencil, then $\Pi_M : \mathbb{R} \rightarrow \mathcal{C}_1$ is a covering map and*

$$P_\nu \circ \Pi_M = \Pi_M \circ \widetilde{B}_e^f, \quad (58)$$

where $f = f(\nu)$ as in (55).

Proof. Given $\nu = (\nu_1, \nu_2)$ obeying (7), we define f by (55). We will use \widehat{M} (47) and T_f (56) to show that the lift of P_ν is a rigid rotation. The expression (25) for π_e^f , gives

$$T_f \circ \pi_e^f(\theta) = \begin{pmatrix} \text{cn}(4K(e)\theta, e) \\ \text{sn}(4K(e)\theta, e) \end{pmatrix}.$$

Since the covering map (57) depends only on the pencil eccentricity e , we can use it for any member of the pencil. Since $T_f|_{E(f)} : E(f) \rightarrow \mathbb{S}^1$ and $\widehat{M}|_{\mathbb{S}^1} : \mathbb{S}^1 \rightarrow \mathcal{C}_1$ are diffeomorphisms and $\pi_e^f : \mathbb{R} \rightarrow E(f)$ is a covering map, then

$$\Pi_M = \widehat{M}|_{\mathbb{S}^1} \circ T_f|_{E(f)} \circ \pi_e^f,$$

is a covering map of \mathcal{C}_1 . Let $\overline{P}_\nu : \mathbb{S}^1 \rightarrow \mathbb{S}^1$ be the circle map given by $\overline{P}_\nu(x, y) = (\widehat{M})^{-1} \circ P_\nu \circ \widehat{M}(x, y)$, for all $(x, y) \in \mathbb{S}^1$. Using Lem. 19 and the fact that \widehat{M} is an orientation-preserving projective transformation, \overline{P}_ν is the Poncelet map with outer ellipse \mathbb{S}^1 and inner ellipse $(\widehat{M})^{-1}(C_\nu) = \mathcal{S}_e^f$. Thus $\overline{P}_\nu = P_e^f$, (54).

We notice that the transformation T_f is linear and orientation-preserving. Given that $E(f) = T_f^{-1}(\mathbb{S}^1)$ and $E(e) = T_f^{-1}(\mathcal{S}_e^f)$, we find that $T_f^{-1} \circ \overline{P}_\nu \circ T_f$ is the Poncelet map with outer ellipse $E(f)$ and inner ellipse $E(e)$. The only possibility is that $T_f^{-1} \circ \overline{P}_\nu \circ T_f = B_e^f$.

Combining these results with Thm. 9 gives the following commutative diagram, where e is the eccentricity of the pencil and $f = f(\nu)$ is given by (55).

$$\begin{array}{ccc}
 \mathbb{R} & \xrightarrow{\tilde{B}_e^f} & \mathbb{R} \\
 \pi_e^f \downarrow & & \downarrow \pi_e^f \\
 E(f) & \xrightarrow{B_e^f} & E(f) \\
 T_f \downarrow & & \downarrow T_f \\
 \mathbb{S}^1 & \xrightarrow{\overline{P}_\nu = P_e^f} & \mathbb{S}^1 \\
 \widehat{M} \downarrow & & \downarrow \widehat{M} \\
 \mathcal{C}_1 & \xrightarrow{P_\nu} & \mathcal{C}_1
 \end{array}
 \quad \begin{array}{l} \Pi_M \\ \Pi_M \end{array}$$

This implies (58). □

We are finally ready to prove Thm. 2 from §1:

Proof of Thm. 2 (Pencil Rotation Number). Lemma 20 implies that if ν is valid (7), then $\tilde{B}_e^f(\theta) = \theta + \hat{\rho}(e, f)$, is a lift of P_ν under the cover Π_M . Recalling the billiard rotation number $\hat{\rho}$ and $\hat{\omega}$ from (4), we can substitute f from (55) to obtain $\omega(\nu) = \hat{\omega}(e, f(\nu))$, which gives (10). This concludes the proof of Thm. 2. □

Remark 17. If we write $B_\nu = \tilde{B}_e^{f(\nu)}$, we get the standard commutative diagram in §1.4. In this case $B_\nu(\theta) = \theta + \hat{\rho}(e, f(\nu)) = \theta + \rho(\nu)$.

Corollary 21. *There exists an equivariant symmetry $\Phi_t : \mathcal{C}_1 \rightarrow \mathcal{C}_1$ such that $P_\nu \circ \Phi_t = \Phi_t \circ P_\nu$, for all $t \in \mathbb{R}$ and all valid ν .*

Proof. For each t , we can define $\Phi_t : \mathcal{C}_1 \rightarrow \mathcal{C}_1$ in terms of the covering map (57) as

$$\Phi_t(\Pi_M(\theta)) = \Pi_M(\theta + t).$$

Given an element $z_0 \in \mathcal{C}_1$, there exists a $\theta_0 \in \mathbb{R}$ such that $z_0 = \Pi_M(\theta_0)$. Then $\Phi_t(z_0) = \Pi_M(\theta_0 + t)$ and $P_\nu(z_0) = \Pi_M(\theta_0 + \rho(\nu))$ and hence

$$P_\nu(\Phi_t(z_0)) = P_\nu(\Pi_M(\theta_0 + t)) = \Pi_M(\theta_0 + t + \rho(\nu)) = \Phi_t(P_\nu(z_0)),$$

for all $t \in \mathbb{R}$. □

5.3 Explicit Rotation Number and Inverse Parameter Conditions

In this section we will prove Thm. 4, thus showing how to solve the inverse problem: given a rotation number, find an element of a pencil whose Poncelet map has that rotation number. As usual we let \mathcal{C}_ν be a pencil (6) of nested ellipses and assume that ν satisfies (7).

Proof of Thm. 4 (Inverse Parameter Conditions). By Lem. 20, the Poncelet map $P_\nu : \mathcal{C}_1 \rightarrow \mathcal{C}_1$ is conjugate to B_e^f , where f is given by (55). The rotation number for the billiard map is $\hat{\rho}(e, f) = \ell \in (0, \frac{1}{2})$ if and only if $f = e \operatorname{cd}(2K(e)\ell, e)$, by Lem. 10. Thus P_ν has rotation number ℓ if and only if

$$\operatorname{cd}^2(2K(e)\ell, e) = \frac{f^2}{e^2} = \frac{\nu_1 + \lambda_3\nu_2}{\nu_1 + \lambda_2\nu_2}. \quad (59)$$

Solving for ν_1/ν_2 , and using standard Jacobi elliptic function identities then gives the promised ratio (13). Since the \mathcal{C}_ν depends only on the ratio ν_1/ν_2 , we can, choose the parameters as

$$\begin{aligned} \nu_1(\ell) &= \lambda_1 \operatorname{cn}^2(2K(e)\ell, e) - \lambda_3, \\ \nu_2(\ell) &= \operatorname{sn}^2(2K(e)\ell, e). \end{aligned} \quad (60)$$

These parameters trace the line segment

$$\nu_1(\ell) + \lambda_1\nu_2(\ell) = \lambda_1 - \lambda_3 \quad (61)$$

that was sketched in Fig. 9. Note that $\nu_2(\ell) > 0$ and $\nu_1(\ell) + \lambda_3\nu_2(\ell) = (\lambda_1 - \lambda_3)\operatorname{cn}^2(2K(e)\ell, e) > 0$. Then Lem. 24 implies that each $\mathcal{C}_{\nu(\ell)}$ is an interior ellipse of the pencil. Thus $P_{\nu(\ell)}$ is conjugate to rigid rotation using the standard covering in Lem. 20. □

This result is similar to the explicit porism given in Lem. 10 for the billiard map, which determined the eccentricity f of the outer ellipse for a given inner ellipse e and rotation number ℓ . As a simple example, we generalize the case $\ell = \frac{1}{4}$ from Ex. 4:

Example 18 (Rotation number $\frac{1}{4}$). Suppose that \mathcal{C}_ν is a pencil of nested ellipses (6) with eigenvalues $\lambda_1 > \lambda_2 > \lambda_3 > 0$. Then the Poncelet map $P_{\nu^*} : \mathcal{C}_1 \rightarrow \mathcal{C}_1$ with

$$\nu^* = \left(\sqrt{(\lambda_1 - \lambda_3)(\lambda_2 - \lambda_3)} - \lambda_3, 1 \right) \quad (62)$$

has rotation number $\rho(\nu^*) = \frac{1}{4}$. We verify this using (10). Substituting ν^* into $\omega(\nu)$ gives

$$\omega(\nu^*) = \arcsin \sqrt{\frac{(\lambda_1 - \lambda_3)}{(\lambda_1 - \lambda_3) + \sqrt{(\lambda_1 - \lambda_3)(\lambda_2 - \lambda_3)}}} = \arcsin \left(\frac{1}{\sqrt{1 + e'}} \right),$$

where we have used the eccentricity (8), and defined $e' = \sqrt{1 - e^2}$. This is identical to the ω computed in Ex. 4, which gives (36) and thus, by (10), $\rho(\boldsymbol{\nu}^*) = \frac{1}{4}$.

Alternatively, a direct use of (60) is possible. Using [BF71, Form. 122.10], we find that

$$\nu_1(1/4) = \lambda_1 \operatorname{cn}^2(\frac{1}{2}K(e), e) - \lambda_3 = \lambda_1 \left(\frac{e'}{1 + e'} \right) - \lambda_3,$$

and

$$\nu_2(1/4) = \operatorname{sn}^2(\frac{1}{2}K(e), e) = \frac{1}{1 + e'}.$$

A simple computation shows that $\boldsymbol{\nu}^* = (1 + e')(\nu_1(1/4), \nu_2(1/4))$, so $\rho(\boldsymbol{\nu}^*) = \frac{1}{4}$.

Given a valid parameter $\boldsymbol{\nu}$, satisfying (7), and a corresponding ellipse $\mathcal{C}_{\boldsymbol{\nu}}$, we can define a *dual* parameter $\bar{\boldsymbol{\nu}}$ so that the Poncelet map for the new ellipse $\mathcal{C}_{\bar{\boldsymbol{\nu}}}$ has a rotation number that “complements” the old rotation number. In particular, this is useful if we want to identify new poristic ellipses.

Theorem 22 (Dual Parameters). *Assume that $\boldsymbol{\nu} = (\nu_1, \nu_2)$ satisfies (7), and define the dual parameter vector*

$$\bar{\boldsymbol{\nu}} = (-\lambda_3\nu_1 + (\lambda_1\lambda_2 - \lambda_1\lambda_3 - \lambda_2\lambda_3)\nu_2, \nu_1 + \lambda_3\nu_2). \quad (63)$$

Then $\bar{\boldsymbol{\nu}}$ satisfies (7), and $\bar{\bar{\boldsymbol{\nu}}} = \delta\boldsymbol{\nu}$, where $\delta = (\lambda_1 - \lambda_3)(\lambda_2 - \lambda_3) > 0$. Moreover, if the Poncelet maps $P_{\boldsymbol{\nu}}$ and $P_{\bar{\boldsymbol{\nu}}}$ have rotation numbers $\rho(\boldsymbol{\nu})$ and $\rho(\bar{\boldsymbol{\nu}})$, respectively, then

$$\rho(\boldsymbol{\nu}) + \rho(\bar{\boldsymbol{\nu}}) = \frac{1}{2}.$$

Thus in particular, $\mathcal{C}_{\boldsymbol{\nu}}$ is poristic if and only if $\mathcal{C}_{\bar{\boldsymbol{\nu}}}$ is poristic.

Proof. The first two assertions are trivial. From the proof of Thm. 4, $\rho(\bar{\boldsymbol{\nu}}) = \ell'$ if and only if (59) holds for the substitutions $\ell \rightarrow \ell'$, $\boldsymbol{\nu} \rightarrow \bar{\boldsymbol{\nu}}$. Substitution of (63) into (59) and simplification then gives

$$\operatorname{cd}^2(2K(e)\ell', e) = \frac{\bar{\nu}_1 + \lambda_3\bar{\nu}_2}{\bar{\nu}_1 + \lambda_2\bar{\nu}_2} = \frac{\lambda_1 - \lambda_3}{\nu_1/\nu_2 + \lambda_1}.$$

If we assume that $\ell' = \frac{1}{2} - \ell$, then [BF71, Form. 122.03] gives

$$\operatorname{cd}(2K(e)(\frac{1}{2} - \ell), e) = \operatorname{sn}(2K(e)\ell, e).$$

Thus we have shown that

$$\operatorname{sn}^2(2K(e)\ell, e) = \frac{\lambda_1 - \lambda_3}{\nu_1/\nu_2 + \lambda_1} \quad \Rightarrow \quad \frac{\nu_1}{\nu_2} = \frac{\lambda_1(1 - \operatorname{sn}^2(2K(e)\ell, e)) - \lambda_3}{\operatorname{sn}^2(2K(e)\ell, e)},$$

which is equivalent to (13). Thus $\rho(\boldsymbol{\nu}) = \ell$, and hence $\rho(\boldsymbol{\nu}) + \rho(\bar{\boldsymbol{\nu}}) = \ell + \frac{1}{2} - \ell = \frac{1}{2}$, as we wanted.³ □

To finish this section, we show that it is possible to identify poristic ellipses using eigenvalues. Suppose that (C_o, C_i) be a pair of matrices satisfying Asm. (SA1)-(SA3) and that $\lambda_1 > \lambda_2 > \lambda_3 > 0$ are the corresponding eigenvalues. If we define the parameters

$$\boldsymbol{\nu}_o = (1, 0), \quad \text{and} \quad \boldsymbol{\nu}_i = (0, 1).$$

³Alternatively, it is possible to show that $\cot(\omega(\bar{\boldsymbol{\nu}})) = \sqrt{1 - e^2} \tan(\omega(\boldsymbol{\nu}))$. Using [BF71, Form. 117.01], we find that $F(\omega(\boldsymbol{\nu}), e) + F(\omega(\bar{\boldsymbol{\nu}}), e) = K(e)$, and therefore $\rho(\boldsymbol{\nu}) + \rho(\bar{\boldsymbol{\nu}}) = \frac{1}{2}$.

then ν_i is valid according to (7) and the ellipses become $C_o = C_{\nu_o}$ and $C_i = C_{\nu_i}$. The dual to ν_i , (63) is then

$$\bar{\nu}_i = (\lambda_1\lambda_2 - \lambda_1\lambda_3 - \lambda_2\lambda_3, \lambda_3).$$

This implies that the pair $(C_o, C_{\bar{\nu}_i})$ also satisfies Asm. (SA1)-(SA3), and has the eigenvalues

$$\bar{\lambda}_1 = \lambda_2(\lambda_1 - \lambda_3), \quad \bar{\lambda}_2 = \lambda_1(\lambda_2 - \lambda_3), \quad \bar{\lambda}_3 = (\lambda_1 - \lambda_3)(\lambda_2 - \lambda_3). \quad (64)$$

In particular, $\bar{\lambda}_1 > \bar{\lambda}_2 > \bar{\lambda}_3 > 0$. Here are several examples using this formula.

Theorem 23. *Let (C_o, C_i) be defined as above so that $C_o^{-1}C_i$ has eigenvalues $\lambda_1 > \lambda_2 > \lambda_3 > 0$. If P_{ν_i} is the corresponding Poncelet map for C_{ν_i} , then we have the following poristic cases.*

1) $\rho(\nu_i) = \frac{1}{4}$ if and only if

$$\lambda_1\lambda_2 - \lambda_1\lambda_3 - \lambda_2\lambda_3 = 0. \quad (65)$$

2) $\rho(\nu_i) = \frac{1}{3}$ if and only if

$$\frac{1}{\sqrt{\lambda_3}} = \frac{1}{\sqrt{\lambda_1}} + \frac{1}{\sqrt{\lambda_2}}. \quad (66)$$

3) $\rho(\nu_i) = \frac{1}{6}$ if and only if

$$\sqrt{1 - \frac{\lambda_3}{\lambda_1}} + \sqrt{1 - \frac{\lambda_3}{\lambda_2}} = 1. \quad (67)$$

Proof. For the first part, we notice that $\rho(\nu_i) = \frac{1}{4}$ if and only if $\rho(\bar{\nu}_i) = \frac{1}{4}$. This happens if and only if ν_i and $\bar{\nu}_i$ are parallel, and hence $\lambda_1\lambda_2 - \lambda_1\lambda_3 - \lambda_2\lambda_3 = 0$. Equivalently, $\nu_i = (0, 1)$ is parallel to ν^* in (62).

Let e be the eccentricity of the pencil (8) and $f = e\sqrt{\lambda_3/\lambda_2}$. We know that $\rho(\nu_i) = \frac{1}{3}$ when e and f solve the polynomial (33). Upon rearrangement this gives $(1 - f^2)(e - f)^2 = f^2(1 - e^2)$, or equivalently

$$\left(\frac{e}{f} - 1\right)^2 = \frac{1 - e^2}{1 - f^2}.$$

Substituting for e and f then implies that $\rho(\nu_i) = \frac{1}{3}$ if and only if

$$\left(\sqrt{\frac{\lambda_2}{\lambda_3}} - 1\right)^2 = \frac{\lambda_2}{\lambda_1},$$

which gives (66) upon rearrangement. Finally, using the dual parameters (63), we know that $\rho(\nu_i) = \frac{1}{6}$ if and only if $\rho(\bar{\nu}_i) = \frac{1}{3}$. Noting that $(C_o, C_{\bar{\nu}_i})$ has the eigenvalues (64) and using these in (66) gives the result (67). \square

Remark 19. Suppose that the generalized characteristic polynomial of the pencil is of the form

$$\det(\lambda C_1 - C_2) = \det(C_1)(\lambda - \lambda_1)(\lambda - \lambda_2)(\lambda - \lambda_3) = \beta_0\lambda^3 + \beta_1\lambda^2 + \beta_2\lambda + \beta_3.$$

As discussed in §1.3, the Cayley condition is computed from the expansion of the square root of this polynomial around $\lambda = 0$, (11). For this case, the Cayley condition becomes

$$\text{Cay}_3 = \alpha_2 = \frac{\sqrt{\beta_3}}{8} \left(4 \left(\frac{\beta_1}{\beta_3} \right) - \left(\frac{\beta_2}{\beta_3} \right)^2 \right).$$

Thus $\rho(\nu_i) = \frac{1}{3}$ if and only if $\alpha_2 = 0$, or $\beta_2^2 = 4\beta_1\beta_3$. Given that $\lambda_1 > \lambda_2 > \lambda_3 > 0$, it is not hard to see that this corresponds exactly with the condition that we found in the theorem above.

Example 20 (Limiting cases). The outer ellipse of the pencil (6) corresponds to the parameter $\nu_o = (1, 0)$. The dual of this point, using the definition (63), is $\bar{\nu}_o = (-\lambda_3, 1)$, on the boundary of (7). This corresponds to the limiting point $\mathcal{C}_{\bar{\nu}_o} = \mathcal{C}_\infty$ (51). Geometrically, it is clear that

$$\rho(\nu_o) = \rho(1, 0) = 0, \quad \rho(\bar{\nu}_o) = \rho(-\lambda_3, 1) = \frac{1}{2}.$$

This verifies that $\rho(\nu_o) + \rho(\bar{\nu}_o) = \frac{1}{2}$.

Example 21 (Euler and Fuss bicentric conditions). When the inner and outer ellipses are circles and the Poncelet map is poristic, the resulting orbit is a ‘‘bicentric polygon’’. The cases of bicentric triangles and quadrilaterals were famously studied by Chapple, Euler, and Fuss [DR11, NA12, CM18]. Here we show that the conditions of Thm. 23 generalize these results. Consider the circles

$$\begin{aligned} \mathcal{C}_1 &= \{(x, y) \in \mathbb{R}^2 : x^2 + y^2 = R^2\}, \\ \mathcal{C}_2 &= \{(x, y) \in \mathbb{R}^2 : (x - a)^2 + y^2 = r^2\}, \end{aligned}$$

where $a, r, R > 0$. Clearly $\mathcal{C}_2 \subset \text{Int}(\mathcal{C}_1)$ when $R > r + |a|$. In particular, this implies that $|a^2 - r^2| < R^2$. These circles can be represented by the pair of matrices

$$C_1 = \begin{pmatrix} 1 & 0 & 0 \\ 0 & 1 & 0 \\ 0 & 0 & -R^2 \end{pmatrix}, \quad C_2 = \begin{pmatrix} 1 & 0 & -a \\ 0 & 1 & 0 \\ -a & 0 & a^2 - r^2 \end{pmatrix}.$$

The characteristic polynomial $\det(\lambda C_1 - C_2)$ has the eigenvalues

$$\lambda_1 = 1, \quad \lambda_{2,3} = \frac{b \pm \sqrt{b^2 - 4r^2R^2}}{2R^2},$$

where $b = R^2 + r^2 - a^2 > 0$. It is easy to see that $\lambda_1 > \lambda_2 > \lambda_3 > 0$.

Using Thm. 23 we can find the relations between a, r and R so that the rotation numbers are $\frac{1}{4}$ and $\frac{1}{3}$. These correspond to bicentric triangles and quadrilaterals, respectively. In particular, (65) gives

$$\lambda_1\lambda_2 - \lambda_1\lambda_3 - \lambda_2\lambda_3 = 0 = \frac{\sqrt{b^2 - 4r^2R^2} - r^2}{R^2}.$$

With some algebra, we find that this holds if and only if

$$\frac{1}{(R - a)^2} + \frac{1}{(R + a)^2} = \frac{1}{r^2},$$

which is precisely the conditions of Fuss.

For rotation number $\frac{1}{3}$, (66) becomes

$$\left(\frac{1}{\sqrt{\lambda_3}} - \frac{1}{\sqrt{\lambda_2}} \right)^2 - \frac{1}{\lambda_1} = 0 = \frac{R(R - 2r) - a^2}{r^2}.$$

With some algebra, we find that this holds if and only if

$$\frac{1}{R - a} + \frac{1}{R + a} = \frac{1}{r}.$$

This is the condition of Chapple-Euler.

Example 22. In this example, we consider a pencil of confocal ellipses generated using the two ellipses

$$\mathcal{Q}_0 = \left\{ (x, y) \in \mathbb{R}^2 : \frac{x^2}{a^2} + \frac{y^2}{b^2} = 1 \right\}, \quad \mathcal{Q}_{\lambda_0} = \left\{ (x, y) \in \mathbb{R}^2 : \frac{x^2}{a^2 - \lambda_0^2} + \frac{y^2}{b^2 - \lambda_0^2} = 1 \right\},$$

where $a > b > \lambda_0 > 0$. These ellipses have foci at $(\pm\sqrt{a^2 - b^2}, 0)$, and the conditions on the parameters imply that \mathcal{Q}_{λ_0} is in the interior of \mathcal{Q}_0 . Using the notation of §4.1, we can represent these using the matrices

$$C_1 = \text{diag}(a^{-2}, b^{-2}, -1), \quad C_2 = \text{diag}((a^2 - \lambda_0^2)^{-1}, (b^2 - \lambda_0^2)^{-1}, -1).$$

Since these are diagonal the three eigenvalues of the pencil are easy to find:

$$\lambda_1 = \frac{b^2}{b^2 - \lambda_0^2}, \quad \lambda_2 = \frac{a^2}{a^2 - \lambda_0^2}, \quad \lambda_3 = 1,$$

where, as usual, we have chosen the labels so that $\lambda_1 > \lambda_2 > \lambda_3 > 0$. For this case the eccentricity e of the pencil is

$$e = \sqrt{\frac{\lambda_1 - \lambda_2}{\lambda_1 - \lambda_3}} = \sqrt{\frac{a^2 - b^2}{a^2 - \lambda_0^2}}.$$

Thus the rotation number for the pencil generated by \mathcal{Q}_0 and \mathcal{Q}_{λ_0} is given by (10) with this eccentricity and eigenvalues. For the case $\nu_i = (0, 1)$, where the inner ellipse is \mathcal{Q}_{λ_0} , this gives

$$\rho(\nu_i) = \frac{F(\arcsin(\lambda_0/b), e)}{2K(e)}.$$

This formula for the rotation number appears in several places in the literature, e.g., [CF88, RR14, DDCRR17] and [KS18, Eq. (8)].

Using the formulas of Thm. 23, we can easily identify the values of λ_0 for for which the corresponding Poncelet map has rotation number $1/3, 1/4$, or $1/6$. For example, (65) implies that $\rho(\nu_i) = 1/4$ if and only if $\lambda_0 = \frac{ab}{\sqrt{a^2 + b^2}}$. Similarly, (67) implies that the rotation number is $1/6$ if and only if $\lambda_0 = \frac{ab}{a+b}$. These conditions of course match those originally found in [RR14].

5.4 Monotonicity

Here we will generalize the results of Lem. 15 to show that the ellipses in the pencil are sequentially nested if the parameter vectors are properly ordered. The following two lemmas will imply Thm. 3, mentioned in the introduction.

Lemma 24. *Assume that C_1, C_2 satisfy Asm. (SA1)-(SA3) and that ν and μ satisfy (7). Then, for the corresponding ellipses $\mathcal{C}_\mu, \mathcal{C}_\nu$,*

$$\mathcal{C}_\mu \subset \text{Int}(\mathcal{C}_\nu) \iff \nu_1\mu_2 - \nu_2\mu_1 > 0,$$

i.e., the cross product $\nu \times \mu > 0$, for the vectors sketched in Fig. 9.

Proof. First, we assume that $\nu_1\mu_2 - \nu_2\mu_1 > 0$. Let $(x, y) \in \mathcal{C}_\mu$ and $\mathbf{u} = (x, y, 1)$. By assumption, $\mathbf{u}^T C_\mu \mathbf{u} = 0$. This implies that $\mathbf{u}^T C_1 \mathbf{u} < 0$ because $\mathcal{C}_\mu \subset \text{Int}(\mathcal{C}_1)$. We will show that $\mathbf{u}^T C_\nu \mathbf{u} < 0$. A simple computation shows that

$$\mu_2 (\mathbf{u}^T C_\nu \mathbf{u}) - \nu_2 (\mathbf{u}^T C_\mu \mathbf{u}) = (\nu_1\mu_2 - \nu_2\mu_1) \mathbf{u}^T C_1 \mathbf{u}.$$

By assumption, $\mu_2 > 0$ and hence $\mathbf{u}^T C_\nu \mathbf{u} < 0$. A similar computation shows the converse. \square

As we noted in Fig. 9, the rotation number is a monotone increasing function along lines in the ν plane that start on the ν_1 -axis and end on the ray $\nu_1 + \lambda_3\nu_2 = 0$. This result follows easily from (10):

Lemma 25. *Let C_1, C_2 and ν, μ be defined as above. Then $\rho(\mu) > \rho(\nu)$ if and only if $\nu \times \mu > 0$.*

Proof. Assume that $\nu \times \mu > 0$. Since the elliptic integral $F(\omega, e)$ in (10) is a monotone increasing function of ω and arcsin is a monotone increasing function on the interval $[0, 1]$, it is sufficient to show that its argument in (10) is also an increasing function. Note that

$$\frac{\mu_2}{\lambda_1\mu_2 + \mu_1} - \frac{\nu_2}{\lambda_1\nu_2 + \nu_1} = \frac{\nu_1\mu_2 - \nu_2\mu_1}{(\lambda_1\nu_2 + \nu_1)(\lambda_1\mu_2 + \mu_1)} > 0,$$

since the denominators above are positive by (7) and $\nu_1\mu_2 - \nu_2\mu_1 > 0$ by assumption. This implies that the argument of the arcsin in (10) is monotone increasing. Thus $\omega(\mu) > \omega(\nu)$, and hence $\rho(\mu) > \rho(\nu)$. The converse is shown in a similar way. \square

Corollary 26. *Two valid parameters μ, ν satisfy $\rho(\mu) = \rho(\nu)$ if and only if they are parallel.*

Together Lem. 24 and Lem. 25 are equivalent to Thm. 3 in §1.

6 Full Poncelet Theorem

As usual, let \mathcal{C}_ν the pencil generated by C_1 and C_2 , so that the parameters ν satisfy (7). In this section we consider compositions of Poncelet maps for different elements of the pencil.

Theorem 27. *Let P_ν, P_μ be Poncelet maps for valid parameters ν, μ , (7). Then*

- 1) $P_\nu \circ P_\mu$ has a lift using the covering Π_M of the form $\theta \mapsto \theta + \rho(\mu) + \rho(\nu)$;
- 2) the maps commute: $P_\nu \circ P_\mu = P_\mu \circ P_\nu$.

Proof. The result follows from Lem. 20. Letting Π_M (57) be the standard covering map, then for each $\theta \in \mathbb{R}$,

$$P_\nu(P_\mu(\Pi_M(\theta))) = P_\nu(\Pi_M(\theta + \rho(\mu))) = \Pi_M(\theta + \rho(\mu) + \rho(\nu)).$$

Clearly, this also implies that P_ν, P_μ commute. \square

Remark 23. Note that Thm. 27 implies Thm. 5 in §1.4 directly.

Example 24. Let $\bar{\nu}$ be the dual of any valid parameter ν , recall Thm. 22. From Thm. 27 the composition $P_{\bar{\nu}} \circ P_\nu$ is a circle map that has rotation number $\frac{1}{2}$. For each pencil, there is only one Poncelet map with that rotation number and it has the limiting point \mathcal{C}_∞ as caustic. Denote this map as $P_\infty = P_{\bar{\nu}} \circ P_\nu$. Since this map has rotation number is $\frac{1}{2}$ the composition

$$P_\infty \circ P_\infty = P_{\bar{\nu}} \circ P_\nu \circ P_{\bar{\nu}} \circ P_\nu = id.$$

This implies that the inverse of P_ν can be written as

$$(P_\nu)^{-1} = P_\infty \circ P_{\bar{\nu}} = P_{\bar{\nu}} \circ P_\infty.$$

An example is sketched in Fig. 10.

As a corollary of these results we have obtained the general theorem of Poncelet.

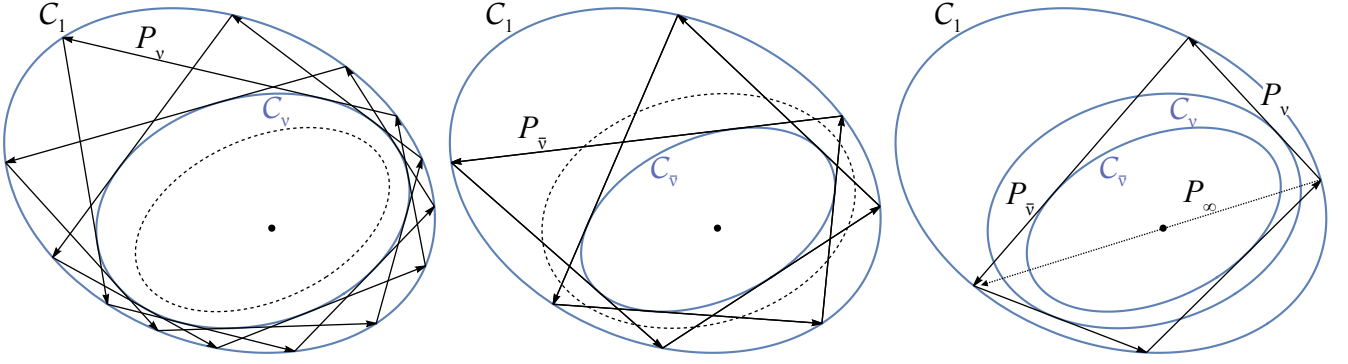


Figure 10: Composition of a Poncelet Map and its dual as in Ex. 24. The left panel shows a map P_ν with $\rho(\nu) = \frac{3}{14}$. The middle panel shows the map $P_{\bar{\nu}}$ with $\rho(\bar{\nu}) = \frac{1}{2} - \rho(\nu) = \frac{2}{7}$. The composition $P_\infty = P_{\bar{\nu}} \circ P_\nu$, shown in the right panel as the dashed line, goes through the limiting ellipse (the point in the figure) and thus has rotation number $\frac{1}{2}$. The pencil for this example has eigenvalues $\{\frac{1}{5}, \frac{1}{8}, \frac{1}{9}\}$, and eccentricity $e = \sqrt{\frac{27}{32}}$ as in Fig. 3, however a different map \widehat{M} (47) was used.

Corollary 28 (Poncelet). *Suppose that $z_0, z_1, \dots, z_N \in \mathcal{C}_1$. Then there exist a sequence of valid parameters $\nu^1, \nu^2, \dots, \nu^N$ and signs $\sigma_1, \sigma_2, \dots, \sigma_N \in \{1, -1\}$ such that,*

- 1) *For each $k = 1, \dots, N$ the segment $\overrightarrow{z_{k-1}z_k}$ is tangent to a unique ellipse \mathcal{C}_{ν^k} . The orientation is positive if $\sigma_k = 1$ and negative if $\sigma_k = -1$.*
- 2) *The Poncelet maps $P_{\nu^k} : \mathcal{C}_1 \rightarrow \mathcal{C}_1$ satisfy $(P_{\nu^k})^{\sigma_k}(z_{k-1}) = z_k$.*
- 3) *If $z_0 = z_N$, then $P_* \equiv (P_{\nu^N})^{\sigma_N} \circ (P_{\nu^{N-1}})^{\sigma_{N-1}} \circ \dots \circ (P_{\nu^1})^{\sigma_1} = \text{id}$.*

Proof. Using the standard covering (57), we can represent the points z_0, \dots, z_N as

$$z_k = \Pi_M(\theta_k),$$

for suitable values of $\theta_k \in \mathbb{R}$. Without loss of generality, we can assume that for each $k = 1, \dots, N$,

$$0 < \ell_k \equiv |\theta_k - \theta_{k-1}| \leq \frac{1}{2},$$

and define $\sigma_k \in \{-1, 1\}$ by

$$\theta_k - \theta_{k-1} = \sigma_k \ell_k.$$

Using (60), we then have

$$\nu^k = (\nu_1(\ell_k), \nu_2(\ell_k)) = (\lambda_1 \text{cn}^2(2K(e)\ell_k, e) - \lambda_3, \text{sn}^2(2K(e)\ell_k, e)).$$

By Thm. 4, P_{ν^k} has rotation number $\rho(\nu^k) = \ell_k$. In fact,

$$(P_{\nu^k})^{\sigma_k}(z_{k-1}) = \Pi_M(\theta_{k-1} + \sigma_k \ell_k) = \Pi_M(\theta_k) = z_k.$$

Recalling Fig. 1, for each $z \in \mathcal{C}_1$, the segment $\overrightarrow{zP_\nu(z)}$ is tangent to \mathcal{C}_ν with positive orientation, and the segment $\overrightarrow{zP_\nu^{-1}(z)}$ is tangent to \mathcal{C}_ν with negative orientation. This implies that the segment $\overrightarrow{z_{k-1}z_k}$ is tangent to \mathcal{C}_{ν^k} , for each k , with positive/negative orientation for $\sigma_k = \pm 1$.

Finally, we notice that

$$\theta_N - \theta_0 = \sum_{k=1}^N (\theta_k - \theta_{k-1}) = \sum_{k=1}^N \sigma_k \ell_k.$$

Consequently, if $z_0 = z_N$, then $\theta_N - \theta_0 \in \mathbb{Z}$, and since $\sum_{k=1}^N \sigma_k \ell_k$ is the rotation number of the composition, we have that the rotation number of P_* is an integer. Consequently P_* is the identity. \square

Remark 25. The symmetry of the Poncelet map can be applied to any finite sequence z_0, \dots, z_N , to give a one-parameter family of orbits that will have the same caustics and orientations as the original. Using the notation of the previous proof, define $\Theta_k(t) = \theta_k + t$ and

$$Z_k(t) = \Pi_M(\Theta_k(t)) = \Phi_t(z_k), \quad (68)$$

where $\Phi_t : \mathcal{C}_1 \rightarrow \mathcal{C}_1$ is the equivariant symmetry of Cor. 21.

Note that, for each t and each k , $\Theta_k(t) - \Theta_{k-1}(t) = \sigma_k \ell_k$. Thus Cor. 28 implies that for each t the segment $\overrightarrow{Z_{k-1}(t)Z_k(t)}$ is tangent to \mathcal{C}_{ν^k} , with the same orientation as $\overrightarrow{z_{k-1}z_k}$. In addition,

$$(P_{\nu^k})^{\sigma_k}(Z_{k-1}(t)) = Z_k(t).$$

Example 26. To illustrate how the equivariant symmetry interacts with Poncelet theorem, Fig. 11 shows a composition of Poncelet maps for a pencil with outer ellipse \mathcal{C}_1 and a pair of inner ellipses \mathcal{C}_{ν^1} and \mathcal{C}_{ν^2} chosen so that the rotation numbers are $\rho(\nu^1) = \ell_1 = \frac{1}{5}$ and $\rho(\nu^2) = \ell_2 = \frac{3}{10}$. In the left panel of Fig. 11 a point z_0 is iterated to obtain the images

$$z_1 = P_{\nu^1}(z_0), \quad z_2 = (P_{\nu^2})^{-1}(z_1), \quad z_3 = P_{\nu^1}(z_2), \quad z_4 = P_{\nu^1}(z_3), \quad z_5 = z_0 = (P_{\nu^2})^{-1}(z_4).$$

Using the notation of the previous corollary, we have $\nu^1 = \nu^3 = \nu^4$, $\nu^2 = \nu^5$, $\sigma_1 = \sigma_3 = \sigma_4 = 1$, and $\sigma_2 = \sigma_5 = -1$. The center and right panels of Fig. 11 show the shape of the orbit with $Z_k(t)$ given by (68) for two values of t .

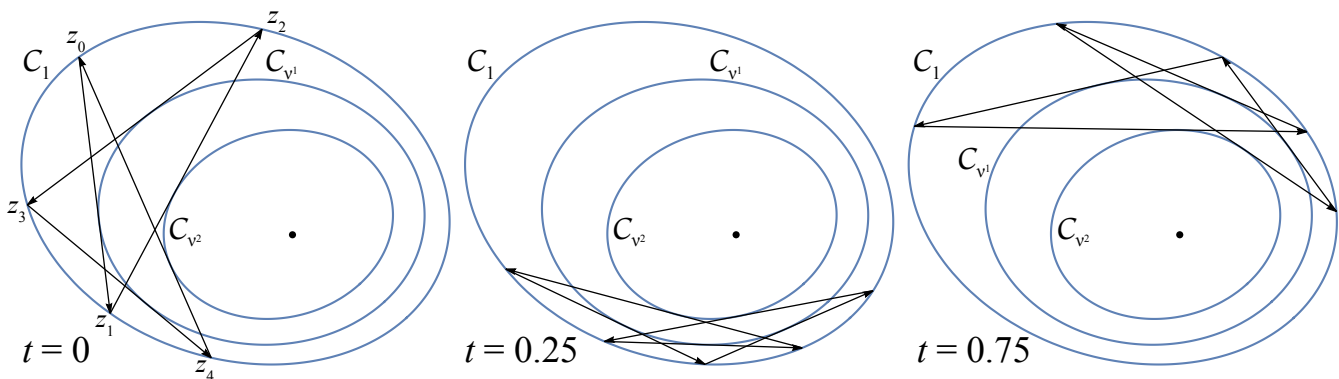


Figure 11: Composition of a pair of Poncelet maps P_{ν^1} and P_{ν^2} with rotation numbers $\frac{1}{5}$ and $\frac{3}{10}$, as in Ex. 26. The resulting map has period 5, so $P_* = id$. The center and right panels show the translations of the orbit for $t = 0.25$ and $t = 0.75$ using the symmetry (68).

Example 27. To illustrate Cor. 28, we choose rotation numbers that are in the real cubic field $\mathbb{Q}(x)$ generated by the single real root of the irreducible polynomial

$$21x^3 + 14x^2 + 7x - 8.$$

The numbers

$$\begin{aligned} \ell_1 &= 3x^3 \approx 0.27910109553533, \\ \ell_2 &= 2x^2 \approx 0.41063584162374, \\ \ell_3 &= x \approx 0.45312020569808 \end{aligned} \quad (69)$$

generate the field, but are irrational and each pair is necessarily incommensurate: there are no integers (m, n, k) for which $m\ell_i + n\ell_j = k$, for $i, j \in \{1, 2, 3\}$. Choosing ν^i using (60), we obtain three Poncelet

maps P_{ν^i} with irrational rotation numbers. For example, the first 90 iterates of an orbit of P_{ν^2} are shown in the left pane of Fig. 12, and 78 iterates of the alternating composition of P_{ν^1} and P_{ν^3} are shown in the middle pane. Neither of these orbits will close, since the corresponding rotation numbers are irrational. However, since $\ell_1 + \ell_2 + \ell_3 = \frac{8}{7}$, the composition $P_{\nu^3} \circ P_{\nu^2} \circ P_{\nu^1}$ has rotation number $\frac{8}{7}$. This map is shown in the right panel of Fig. 12. Defining z_k as in Cor. 28, we see that $z_{21} = z_0$ for any starting point.

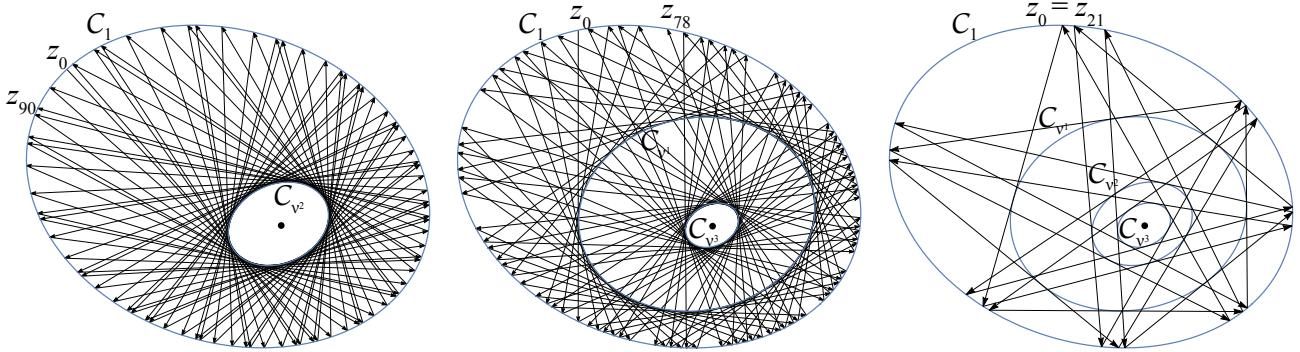


Figure 12: Poncelet maps with rotation numbers in a cubic field as discussed in Ex. 27. (Left) The map P_{ν^2} with rotation number ℓ_2 (69). (Middle) The map $P_{\nu^3} \circ P_{\nu^1}$ with rotation number $\ell_3 + \ell_1$. Since the rotation numbers are incommensurate, there is no combination of only two of the maps, P_{ν^1} , P_{ν^2} , P_{ν^3} , that will be poristic. (Right) The map $P_{\nu^3} \circ P_{\nu^2} \circ P_{\nu^1}$ with rotation number $\frac{8}{7}$. Here the pencil is the same as that in Fig. 10.

7 Conclusions

In this paper we have studied Poncelet's theorem from a dynamical systems point of view. In §2 we analyzed elliptic billiard maps and found a formula for the rotation number. We began by recalling the known symmetry of the elliptic billiard that implies its integrability. This symmetry gives a conjugacy for each orbit with an inner elliptical caustic to a map that is a rigid translation on a covering space. This resulted in an explicit expression for the rotation number of the circle maps corresponding to Poncelet dynamics for the case of confocal ellipses. The rotation number was written in terms of Jacobi elliptic functions with modulus equal to the eccentricity of the inner ellipse, recall (4).

We showed in §5 that there is a conjugacy between the confocal case and the general Poncelet map for elements of a pencil of ellipses. As we noted in §4, the fundamental parameters of such a pencil are its three eigenvalues. In particular, these determine the eccentricity of the pencil, (8), which again appears as the modulus of the elliptic functions that give the rotation number for any element of the pencil, (10). In Thm. 4 we obtained an explicit form for the choice of pencil element that gives a Poncelet map with a given rotation number.

When the rotation number is rational, all orbits of the Poncelet map are periodic. These continuous families of polygons are known as Poncelet porisms. Using the explicit form of the rotation number, we reproduced well-known explicit expressions for some of the low period porisms that arise from the classical conditions of Cayley, both for the confocal case in §3 and for general pencils in §5.3. We found that the conditions for porisms can be written solely in terms of the eigenvalues of the pencil.

Finally, in §6 we showed how the general Poncelet theorem, for maps with an arbitrary sequence of inner ellipses chosen from a pencil, follows from the fact that a single covering space simplifies all the Poncelet maps in a pencil. We gave an explicit expression (57) for the covering space in terms of the projective map (47) and the pencil eccentricity (8).

Appendices

A Confocal Poristic Examples

In this appendix we recall two classical formulas for Poristic ellipses. We consider a pair of confocal ellipses $E(e)$ and $E(f)$ with eccentricities e and f so that $0 < f < e < 1$.

A.1 Rotation number $\frac{1}{3}$

We can show that the rotation number is $\frac{1}{3}$ when the eccentricities are in the set (33). To find such a pair of ellipses we should find an orbit whose segments form a triangle. Consider the three points

$$\begin{aligned} z_0 &= \frac{1}{e} \left(1, -\frac{1}{f} \sqrt{(1-f^2)(e^2-f^2)} \right), \\ z_1 &= \frac{1}{e} \left(1, \frac{1}{f} \sqrt{(1-f^2)(e^2-f^2)} \right), \\ z_2 &= \left(-\frac{1}{f}, 0 \right), \end{aligned}$$

on $E(f)$. Clearly, the directed segment $\overrightarrow{z_0 z_1}$ is tangent to the $E(e)$ at $(\frac{1}{e}, 0)$. To produce a triangle, we need to adjust e so that both segments $\overrightarrow{z_1 z_2}$ and $\overrightarrow{z_2 z_0}$ are tangent to $E(e)$. To solve this problem, substitute the segment $(1-t)z_1 + tz_2$ into $E(e)$ to give the function

$$h(t) = e^2((1-t)x_1 + tx_2)^2 + \left(\frac{e^2}{1-e^2} \right) ((1-t)y_1 + ty_2)^2 - 1.$$

The segment $\overrightarrow{z_1 z_2}$ is tangent to $E(e)$ if and only if h has a double root in the interval $(0, 1)$, so that the discriminant of h is necessarily zero—this is exactly (33). We conclude that the segment $\overrightarrow{z_1 z_2}$ is tangent to $E(e)$ if and only if (33) is satisfied. By symmetry, $\overrightarrow{z_2 z_0}$ is also tangent to $E(e)$. This implies that $\{z_0, z_1, z_2\}$ is an orbit of B_e^f and hence $\hat{\rho}(e, f) = 1/3$.

A.2 Cayley's Solution for Period-5 orbits

As mentioned in §1.3, the zero level sets of the polynomial Cay_N correspond to Poncelet porisms with period N [GH78, DR98a, DR98b]. If $N = 5$, the result allows us to compute a polynomial $\text{Cay}_5(e, f)$ such that

$$\text{Cay}_5^{-1}\{0\} \cap \Delta = \Delta_{1/5} \cup \Delta_{2/5}.$$

If the sets $\Delta_{1/5}$ and $\Delta_{2/5}$ can be written as zeros of polynomials, then they have to be factors of Cay_5 . Using symbolic manipulation, we found

$$\begin{aligned} \Delta_{1/5} &= \{(e, f) \in \Delta : e^6 + 8e^5 f^5 - 10e^5 f^3 + 2e^5 f - 4e^4 f^6 + 5e^4 f^4 \\ &\quad - 4e^4 f^2 - 12e^3 f^7 + 12e^3 f^5 + 4e^2 f^{10} - 5e^2 f^8 \\ &\quad + 4e^2 f^6 - 2ef^{11} + 10ef^9 - 8ef^7 - f^{12} = 0\}, \\ \Delta_{2/5} &= \{(e, f) \in \Delta : e^6 - 8e^5 f^5 + 10e^5 f^3 - 2e^5 f - 4e^4 f^6 + 5e^4 f^4 \\ &\quad - 4e^4 f^2 + 12e^3 f^7 - 12e^3 f^5 + 4e^2 f^{10} - 5e^2 f^8 \\ &\quad + 4e^2 f^6 + 2ef^{11} - 10ef^9 + 8ef^7 - f^{12} = 0\}. \end{aligned}$$

Using formula (37), we can verify numerically that $\Delta_{1/5}$ and $\Delta_{2/5}$ are the poristic sets.

B Asymptotic Limits

For each $0 < f < 1$ we want to show that

$$\lim_{e \rightarrow 1^-} \hat{\rho}(e, f) = \frac{1}{2},$$

as mentioned in Rem. 3. By Thm. 1, for each $f < e < 1$,

$$0 < \frac{1}{2} - \hat{\rho}(e, f) = \frac{K(e) - F(\hat{\omega}(e, f), e)}{2K(e)} = \frac{1}{2K(e)} \int_{\hat{\omega}(e, f)}^{\pi/2} \frac{d\tau}{\sqrt{1 - e^2 \sin^2 \tau}},$$

where $\hat{\omega}(e, f)$ is given in (4). The denominator in the integral above is monotone decreasing on $[0, \pi/2]$, with a minimum value of $\sqrt{1 - e^2}$. Therefore,

$$\left| \frac{1}{2} - \hat{\rho}(e, f) \right| \leq \frac{1}{2K(e)} \left(\frac{\pi/2 - \hat{\omega}(e, f)}{\sqrt{1 - e^2}} \right).$$

A simple computation then gives

$$\lim_{e \rightarrow 1^-} \frac{\pi/2 - \hat{\omega}(e, f)}{\sqrt{1 - e^2}} = \frac{\sqrt{1 - f^2}}{f} < \infty.$$

Therefore, since $K(e) \rightarrow \infty$, as $e \rightarrow 1^-$, we conclude that $\lim_{e \rightarrow 1^-} \hat{\rho}(e, f) = \frac{1}{2}$.

In Rem. 5, we mentioned the following limit

$$\lim_{e \rightarrow 1^-} e \operatorname{cd}(2K(e)\ell, e) = 1.$$

This can be shown, using results in [CT83, Thm. 3] and [Sv16, Lem. 2]. In fact, fixing $\ell \in (0, 1/2)$, we have the following asymptotic expansions, as $e \rightarrow 1^-$.

$$\operatorname{cn}(2K(e)\ell, e) = 2^{1-\ell}(1 - e^2)^\ell + o\left((1 - e^2)^\ell\right),$$

$$\operatorname{dn}(2K(e)\ell, e) = 2^{1-\ell}(1 - e^2)^\ell + o\left((1 - e^2)^\ell\right).$$

These imply the limit above.

C Derivatives of the billiard rotation number

To show that the rotation number is a monotone function of e and f , we first obtain some related results for elliptic functions. The *Jacobi epsilon function* is defined as

$$\mathcal{E}(u, e) = \int_0^u \operatorname{dn}^2(\tau, e) d\tau = E(\operatorname{am}(u, e), e),$$

where E is the incomplete elliptic integral of the second kind,

$$E(\phi, e) = \int_0^\phi \sqrt{1 - e^2 \sin^2 \tau} d\tau.$$

In particular, the complete elliptic integral of the second kind becomes $\mathcal{E}(K(e), e) = E(\pi/2, e)$. We first prove the following auxiliary result.

Lemma 29. *Let $z, e \in (0, 1)$ and define $g(z) \equiv \mathcal{E}(zK(e), e) - z\mathcal{E}(K(e), e)$. Then $g(z) > 0$.*

Proof. The second derivative of g is

$$g''(z) = -2e^2 K^2(e) \operatorname{dn}(zK(e), e) \operatorname{cn}(zK(e), e) \operatorname{sn}(zK(e), e).$$

Since $z \in (0, 1)$ then $g''(z) < 0$, so g is strictly concave on $(0, 1)$. Moreover, given that $g(0) = g(1) = 0$, then $g(z) > 0$, for all $z \in (0, 1)$. \square

To prove the next lemma, we will use derivatives of the elliptic functions and integrals with respect to the argument and modulus, as found in [BF71, Formulas 710.00, 710.61, 731.11]:

$$\begin{aligned} \frac{\partial}{\partial e} K(e) &= \frac{1}{e(1-e^2)} [\mathcal{E}(K(e), e) - (1-e^2)K(e)], \\ \frac{\partial}{\partial e} \operatorname{cd}(t, e) &= \frac{\operatorname{sn}(t, e)}{e \operatorname{dn}^2(t, e)} [\mathcal{E}(t, e) - (1-e^2)t], \\ \frac{\partial}{\partial t} \operatorname{cd}(t, e) &= -(1-e^2) \frac{\operatorname{sn}(t, e)}{\operatorname{dn}^2(t, e)}. \end{aligned} \tag{70}$$

Lemma 30. *Defining $f(\ell, e)$ as in (37), then $\frac{\partial f}{\partial \ell} < 0$ and $\frac{\partial f}{\partial e} > 0$.*

Proof. To clarify the notation let $R : (0, 1/2) \times (0, 1) \rightarrow \mathbb{R}$ be the function

$$R(\ell, e) = e \operatorname{cd}(2K(e)\ell, e), \tag{71}$$

given in (37). Using (70), we find

$$\begin{aligned} \frac{\partial R}{\partial \ell} &= -2e(1-e^2) \frac{\operatorname{sn}(2K(e)\ell, e)}{\operatorname{dn}^2(2K(e)\ell, e)} K(e), \\ \frac{\partial R}{\partial e} &= \operatorname{cd}(2K(e)\ell, e) + \frac{\operatorname{sn}(2K(e)\ell, e)}{\operatorname{dn}^2(2K(e)\ell, e)} [\mathcal{E}(2K(e)\ell, e) - 2\ell \mathcal{E}(K(e), e)]. \end{aligned}$$

If $\ell \in (0, 1/2)$, then cd , sn , and dn are positive with the arguments above. Using Lem. 29, we find that $\mathcal{E}(2K(e)\ell, e) - 2\ell \mathcal{E}(K(e), e) > 0$. Since (37) implies that $f = R(\ell, e)$, we conclude that $\frac{\partial f}{\partial \ell} < 0$ and $\frac{\partial f}{\partial e} > 0$. \square

Lemma 31. *The billiard rotation number $\hat{\rho}(e, f)$ given by (4) satisfies $\frac{\partial \hat{\rho}}{\partial e} > 0$ and $\frac{\partial \hat{\rho}}{\partial f} < 0$.*

Proof. Using (71) together with (37) gives the implicit expression

$$R(\hat{\rho}(e, f), e) = f.$$

This implies that

$$\frac{\partial R}{\partial \ell} \cdot \frac{\partial \hat{\rho}}{\partial e} + \frac{\partial R}{\partial e} = 0, \quad \frac{\partial R}{\partial \ell} \cdot \frac{\partial \hat{\rho}}{\partial f} = 1.$$

Since $\frac{\partial R}{\partial \ell} < 0$ and $\frac{\partial R}{\partial e} > 0$, this implies the result. \square

References

- [BF71] P.F. Byrd and M.D. Friedman. *Handbook of elliptic integrals for engineers and scientists*. Die Grundlehren der mathematischen Wissenschaften, Band 67. Springer-Verlag, New York-Heidelberg, 1971. Second edition, revised.
- [BKOR87] H.J.M. Bos, C. Kers, F Oort, and D.W. Raven. Poncelet’s closure theorem. *Expositiones Mathematicae*, 5(4):289–364, 1987.
- [BZ12] V.P. Burskii and A.S. Zhedanov. On Dirichlet, Poncelet and Abel problems. *Comm. Pure Applied Analysis*, 12(4):1587–1633, 2012. <https://doi.org/10.3934/cpaa.2013.12.1587>.
- [CF88] S.-J. Chang and R. Friedberg. Elliptical billiards and Poncelet’s theorem. *J. Math. Physics*, 29(7):1537–1550, 1988. <https://doi.org/10.1063/1.527900>.
- [CFS82] I.P. Cornfeld, S.V. Fomin, and Ya.G. Sinai. *Ergodic Theory*, volume 245 of *Grundlehren Der Mathematischen Wissenschaften*. Springer-Verlag, New York, 1982.
- [CGM10] A. Cima, A. Gasull, and V. Mañosa. On Poncelet’s maps. *Computers & Mathematics with Applications*, 60(5):1457–1464, 2010. <https://doi.org/10.1016/j.camwa.2010.06.027>.
- [CM16] W. Cieślak and W. Mozgawa. In search of a measure in Poncelet’s porism. *Acta Math. Hungar.*, 149(2):338–345, 2016. <https://doi.org/10.1007/s10474-016-0620-3>.
- [CM18] W. Cieślak and W. Mozgawab. The Fuss formulas in the Poncelet porism. *Computer Aided Geometric Design*, 66:19–30, 2018.
- [CS10] W. Cieślak and E. Szczygielska. On Poncelet’s porism. *Universitatis Mariae Curie-Skłodowska Lublin – Polonia Annales*, Lxiv(2):21–28, 2010. <https://doi.org/10.2478/v10062-010-0011-0>.
- [CT83] B. C. Carlson and J Todd. The degenerating behavior of elliptic functions. *SIAM Journal on Numerical Analysis*, 20(6):1120–1129, 1983. <http://www.jstor.org/stable/2157146>.
- [DDCRR17] J. Damasceno, M.J. Dias Carneiro, and R. Ramírez-Ros. The billiard inside an ellipse deformed by the curvature flow. *Proc. Amer. Math. Soc.*, 145(2):705–719, 2017.
- [DLM12] H.R. Dullin, H.E. Lomeli, and J.D. Meiss. Symmetry reduction by lifting for maps. *Nonlinearity*, 25:1709–1733, 2012. <https://doi.org/10.1088/0951-7715/25/6/1709>.
- [DR98a] V. Dragovič and M. Radnovič. Conditions of Cayley’s type for ellipsoidal billiard. *J. Math. Phys.*, 39(1):355–362, 1998. <https://doi.org/10.1063/1.532317>.
- [DR98b] V. Dragovič and M. Radnovič. On periodical trajectories of the billiard systems within an ellipsoid in R^d and generalized Cayley’s condition. *J. Math. Phys.*, 39(11):5866–5869, 1998. <https://doi.org/10.1063/1.532600>.
- [DR06] V. Dragovič and M. Radnovič. A survey of the analytical description of periodic elliptical billiard trajectories. *Journal of Mathematical Sciences*, 135(4):3244–3255, 2006. <https://doi.org/10.1007/s10958-006-0154-2>.
- [DR10] V.I. Dragovič and M. Radnovič. Integrable billiards and quadrics. *Russian Mathematical Surveys*, 65(2):319–379, 2010. <http://dx.doi.org/10.1070/RM2010v065n02ABEH004673>.

- [DR11] V. Dragović and M. Radnović. *Poncelet Porisms and Beyond: Integrable Billiards, Hyperelliptic Jacobians and Pencils of Quadrics*. Frontiers in Mathematics. Birkhäuser, 2011. <https://doi.org/10.1007/978-3-0348-0015-0>.
- [DR14] V. Dragović and M. Radnović. Bicentennial of the great Poncelet theorem (1813–2013): Current advances. *Bull. Amer. Math. Soc*, 51(3):373–445, 2014. <https://www.ams.org/journals/bull/2014-51-03/S0273-0979-2014-01437-5/>.
- [Fla09] L. Flatto. *Poncelet’s Theorem*. AMS, 2009. <https://doi.org/10.1090/mbk/056>.
- [FT07] D. Fuchs and S. Tabachnikov. *Mathematical Omnibus: Thirty Lectures on Classic Mathematics*. AMS, 2007. <https://bookstore.ams.org/mbk-46>.
- [Gar19] A. Garcia. Elliptic billiards and ellipses associated to the 3-periodic orbits. *Am. Math. Mon.*, 126(6):491–504, 2019. <https://doi.org/10.1080/00029890.2019.1593087>.
- [GH77] P.J. Griffiths and J. H. Harris. A Poncelet theorem in space. *Commentarii Mathematici Helvetici*, 52(1):145–160, 1977. <https://doi.org/10.1007/BF02567361>.
- [GH78] P.J. Griffiths and J. H. Harris. On Cayley’s explicit solution to Poncelet porism. *Enseign. Math., Ser.2*, 14(1-2):31–40, 1978. <http://publications.ias.edu/node/221>.
- [GR65] I.S. Gradshteyn and I.M. Ryzhik. *Table of Integrals Series and Products*. Academic Press, New York, 1965.
- [GR21] R.A. Garcia and D.S. Reznik. *Discovering Poncelet Invariants in the Plane*. Books in Bytes. IMPA, Rio de Janeiro, 2021.
- [KKG10] J.-S. Kim, P. Gurdjos, and I.S. Kweon. Euclidean structure from confocal conics: Theory and application to camera calibration. *Computer Vision and Image Understanding*, 114(7):803–812, 2010. <https://doi.org/10.1016/j.cviu.2010.03.004>.
- [Kol85] R. Kolodziej. The rotation number of some transformation related to billiards in an ellipse. *Studia Mathematica*, LXXXI:293–302, 1985. <http://matwbn.icm.edu.pl/ksiazki/sm/sm81/sm81125.pdf>.
- [KS18] V. Kaloshin and A. Sorrentino. On the local Birkhoff conjecture for convex billiards. *Annals of Math.*, 188:315–380, 2018.
- [Lom96] H.E. Lomelí. Perturbations of elliptic billiards. *Physica D*, 99(1):59–80, 1996. [https://doi.org/10.1016/S0167-2789\(96\)00061-9](https://doi.org/10.1016/S0167-2789(96)00061-9).
- [LT07] M. Levi and S. Tabachnikov. The Poncelet grid and billiards in ellipses. *The American Mathematical Monthly*, 114(10):895–908, 2007. <http://www.jstor.org/stable/27642362>.
- [Mei92] J.D. Meiss. Symplectic maps, variational principles, and transport. *Rev. Mod. Phys.*, 64(3):795–848, 1992. <https://doi.org/10.1103/RevModPhys.64.795>.
- [Mir10] B. Mirman. Short cycles of Poncelet’s conics. *Linear Algebra and its Applications*, 432(10):2543–2564, 2010. <https://doi.org/10.1016/j.laa.2009.11.032>.
- [Mir12] B. Mirman. Explicit solutions to Poncelet’s porism. *Linear Algebra and its Applications*, 436(9):3531–3552, 2012. <https://doi.org/10.1016/j.laa.2011.12.024>.

- [NA12] B.T. Nohara and A. Arimoto. Some relations of Poncelet's porism for two ellipses. *Proc. Japan Academy, Series A*, 88(6):85–90, 2012. <https://doi.org/10.3792/pjaa.88.85>.
- [Och11] K. Ochs. A comprehensive analytical solution of the nonlinear pendulum. *European Journal of Physics*, 32(2):479–490, 2011. <https://doi.org/10.1088/0143-0807/32/2/019>.
- [Par98] B. N. Parlett. *The General Linear Eigenvalue Problem*, volume 20 of *Classics in Applied Mathematics*, chapter 15, pages 339–368. Society for Industrial and Applied Mathematics, 1998. <https://epubs.siam.org/doi/abs/10.1137/1.9781611971163.ch15>.
- [RR14] Rafael Ramírez-Ros. On Cayley conditions for billiards inside ellipsoids. *Nonlinearity*, 27:1003–1028, 2014.
- [SS90] G. W. Stewart and Ji Guang Sun. *Matrix perturbation theory*. Computer Science and Scientific Computing. Academic Press, Inc., Boston, MA, 1990.
- [Sv16] Petr Siegl and František Štampach. On extremal properties of Jacobian elliptic functions with complex modulus. *J. Math. Anal. Appl.*, 442(2):627–641, 2016.
- [Tab93] S. Tabachnikov. Poncelet's theorem and dual billiards. *L'enseignement Mathématique*, 39, 1993. <http://dx.doi.org/10.5169/seals-60421>.